Received: 3 January 2017 | Revised: 14 March 2018 | Accepted: 14 March 2018

DOI: 10.1002/gea.21684

RESEARCH ARTICLE

WILEY Geoarchaeology An International Journal

Geochemistry of Byzantine and Early Islamic glass from Jerash, Jordan: Typology, recycling, and provenance

Gry Hoffmann Barfod[1,2] | Ian C. Freestone[3] | Achim Lichtenberger[4] | Rubina Raja[1] | Holger Schwarzer[4]

[1]Centre of Excellence Urban Network Evolutions, Aarhus Universitet, Aarhus, Denmark

[2]Department of Geoscience, Aarhus University, Aarhus, Denmark

[3]Institute of Archaeology, UCL, London, UK

[4]Institut für Klassische Archäologie und Christliche Archäologie, Münster University, Münster, Germany

Correspondence
Rubina Raja, Centre of Excellence Urban Network Evolutions, Aarhus Universitet, Aarhus, Denmark.
Email: rubina.raja@cas.au.dk

Funding information
Carlsbergfondet; Deutsche Forschungsgemeinschaft, Grant/Award Number: LI-978/4-2; EliteForsk Award; Deutscher Palästina-Verein; Danmarks Grundforskningsfond, Grant/Award Number: 119

Scientific editing by Drew Coleman

Abstract

Twenty-two objects of glass from the Decapolis city of Gerasa, N. Jordan, with characteristic vessel forms ranging from Hellenistic to Early Islamic (2nd century BCE to 8th century CE) were analyzed for major and trace elements, and 16 samples for Sr-isotopes. The majority were produced in the vicinity of Apollonia on the Palestine coast in the 6th–7th centuries CE, and strong inter-element correlations for Fe, Ti, Mn, Mg, Nb reflect local variations in the accessory minerals in the Apollonia glassmaking sand. The ubiquity of recycling is reflected in elevated concentrations and high coefficients of variation of colorant-related elements as well as a strong positive correlation between K and P. The high level of K contamination is attributed to the use of pomace (olive processing residue) as fuel, and a negative correlation with Cl, due to volatilization as the glass was reheated. This points to an efficient system for the collection of glass for recycling in Jerash during the latter part of the first millennium CE. Differences in elemental behavior at different sites in the Levant may reflect the context of the recycling system, for example, glass from secular contexts may contain less colorants derived from mosaics than glass associated with churches.

KEYWORDS

Apollonia, Byzantine glass, Early Islamic glass, EMP, Gerasa, Jerash, LA-ICP-MS, Levantine, MC-ICP-MS, olive fuel, provenance, recycling, Sr isotope, trace elements, trade, typology

1 | INTRODUCTION

It is now generally accepted that from the late first millennium BCE until the late first millennium CE, the ancient glass industry was centralized. Large-scale natron glass production supplying the entire Eastern Mediterranean region was centered in only a few locations along the Palestine coast and in Egypt. Each production center produced unique glasses due to minor differences in recipe and the local raw materials, but common for the natron glass types is that they were made by mixing calcium carbonate-bearing sand with natron (soda) from salt lakes at Wadi el-Natrun or the Nile Delta (e.g., Brill, 1988; Degryse, 2014; Degryse & Schneider, 2008; Freestone, Gorin-Rosen, & Hughes, 2000; Freestone, Leslie, Thirlwall, & Gorin-Rosen, 2003; Nenna, Vichy, & Picon, 1997). These primary glassmaking centers exported the raw glass to population centers across the ancient world where secondary glass workshops remelted and shaped the raw material into vessels, windows, and jewelry. Whereas the general outline of this substantial industry is accepted, issues such as variability with region, chronology, social and economic context, and the role of recycling remain to be elucidated (Rehren & Freestone, 2015). The present paper provides indicative results for a major city in the Levant.

The modern town of Jerash, located about 50 km from Jordan's modern capital Amman, is the site of the ancient city of Gerasa (Figure 1). The city, which during the Roman period belonged to the Decapolis (Pliny, *Natural History*, 36.45), prospered during the first millennium CE until an earthquake in 749 CE led to its demise and abandonment. The site has been investigated for more than 100 years. In particular, Yale University conducted large-scale excavations here in the 1920s, published in the monumental work of Kraeling (1938). Several find groups were studied, but only little comprehensive work exists on the typology and chemistry of Gerasa glass (Arinat, Shiyyab, & Abd-Allah, 2014; Meyer, 1988).

The Danish–German Jerash Northwest Quarter Project has been on-going since 2011 and investigates the settlement history of the

This is an open access article under the terms of the Creative Commons Attribution License, which permits use, distribution and reproduction in any medium, provided the original work is properly cited.

© 2018 The Authors *Geoarchaeology* Published by Wiley Periodicals, Inc.

FIGURE 1 Regional map of Syria–Palestine with location of the study site of Jerash as well as surrounding contemporary cities of Petra and Umm el-Jimal. Also shown are glass production sites along the Levantine coast at Apollonia, Jalame, and Bet Eli'ezer [Color figure can be viewed at wileyonlinelibrary.com]

highest area within the walled city (Lichtenberger & Raja, 2015, 2017) (Figure 2). The project explores mainly domestic complexes of this quarter of the city. Most of the excavated structures stem from the Late Roman to Early Islamic periods. During the excavations, evidences were excavated containing the inventory of houses and among the finds were glass vessels, most of them fragmented. Here, we present major and trace elements for 22 as well as Sr isotopic compositions for 16 glass artefacts excavated during the 2013 campaign of this project, selected to represent the range of glass forms encountered. The objectives of this study are twofold. The first is to determine the main glass types that reached Gerasa and how this reflects the supplies into the city and thus regional trade networks. The second objective is a detailed characterization of the contaminants and postproduction chemical signatures that became incorporated into the glasses during remelting in secondary glass workshops. The signatures provide clues about the local remelting techniques, furnaces, fuel sources, glass types mixed during melting and/or added colorants which, ultimately, reflect the inner workings and infra-structure of Gerasa within a local and regional context.

2 | SAMPLE MATERIAL

During the 2013 campaign of the Danish–German Jerash Northwest Quarter Project, almost 300 glass items, mostly very fragmented, were excavated from trenches D–H (Figure 2); most stem from the Middle–Late Roman and Byzantine–Early Islamic periods. The vessels were predominantly free-blown. Most Hellenistic, Roman, and Byzantine fragments were found in secondary strata mixed with other materials and their original contexts therefore lost.

The glass fragments for analysis were chosen to provide a broad typological span of diagnostic and datable forms to study long term developments in glass consumption and recycling purposes within

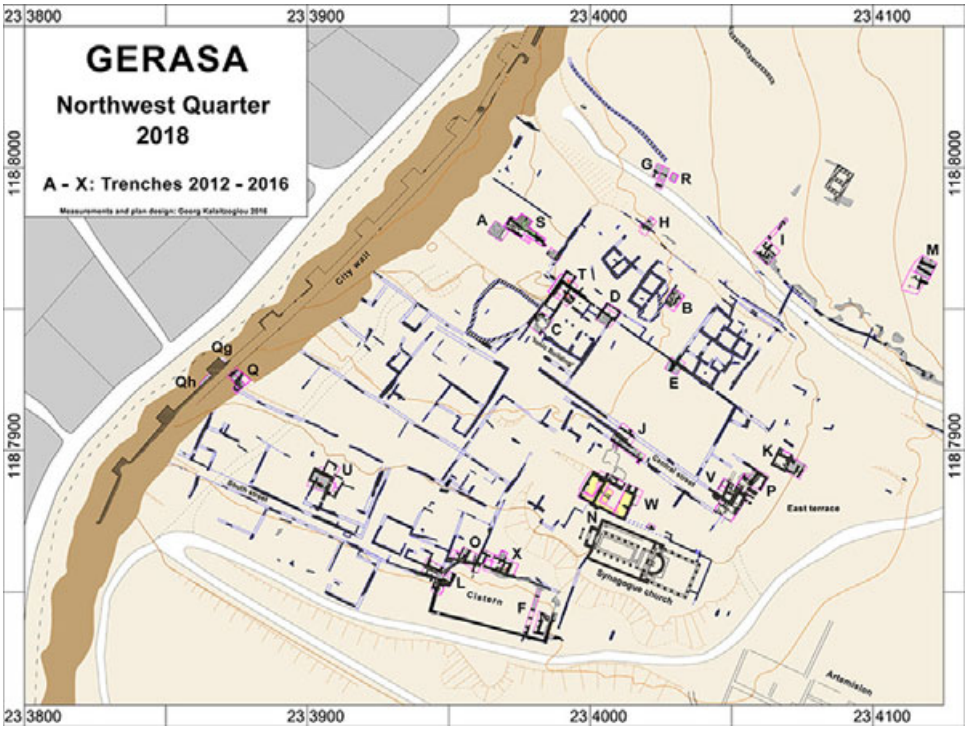

FIGURE 2 Excavated areas in the Northwest Quarter of Jerash. The glass analyzed in this study was recovered from trenches D–H. Two of the trenches lie in the central area of the Northwest Quarter (D, E), one is on the southern slope (F) and two are on the northern slope (G, H) [Color figure can be viewed at wileyonlinelibrary.com]

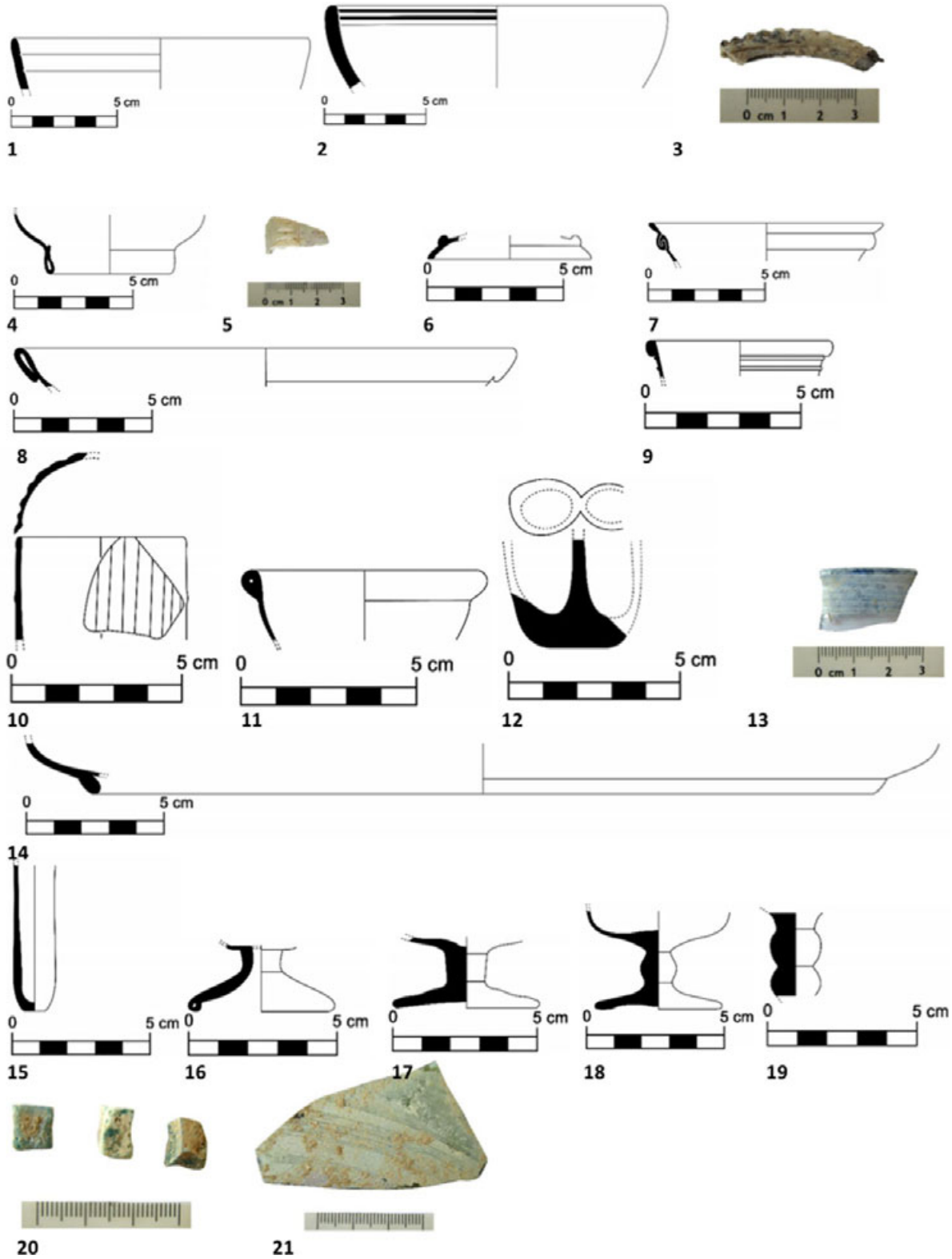

FIGURE 3 Glass samples 1–21 used in the study. Note that two fragments from object 11 (11a and 11b) were analysed [Color figure can be viewed at wileyonlinelibrary.com]

Jerash. Glass descriptions, typologies, and deduced chronologies are presented in Figure 3 and details listed in Supplemental Table 1. The chosen glass samples are not quantitatively representative for all periods of occupation, since the majority of glass fragments from the Northwest Quarter excavations stems from the Byzantine and Early Islamic periods (5th–8th centuries CE) but we have included earlier representative forms in the analytical sample set.

Early period material is rarely encountered among the glass finds. Only a few sherds can be assigned to the Hellenistic period (336 BC–30 BC). They belong to cast grooved bowls showing a

TABLE 1 Composition of Corning B glass standard by electron microprobe in this study compared to recommended composition

	SiO_2	Na_2O	CaO	Al_2O_3	K_2O	MgO	P_2O_5	TiO_2	FeO	MnO	Cl	SO_2	CuO	PbO	Total
Corning B															
Recommended values[a]	61.55	17.00	8.56	4.36	1.00	1.03	0.82	0.09	0.31	0.25	0.20	0.45	2.66	0.50	
Measured[b]	62.17	17.37	8.92	4.29	1.08	1.03	0.80	0.12	0.33	0.24	0.17	0.37	2.90	0.48	100.2
2 Standard Deviation	0.39	0.27	0.16	0.18	0.05	0.04	0.06	0.02	0.05	0.04	0.02	0.02	0.17	0.16	
Relative difference	−1.0%	−2.2%	−4.2%	1.6%	−8.0%	0.0%	2.4%	−33%	−6.5%	4.0%	15%	18%	−9.0%	4.0%	

[a]Recommended values from Brill (1999), except PbO and SO_2 from Vicenzi et al. (2002).
[b]Average of 20 analyses during multiple analytical sessions.

conical or hemispherical shape (cat. nos. 1–2). The Early Roman imperial period is absent, as are typical forms of the 1st and early 2nd centuries CE. The majority of the Roman glass vessels—as far as can be determined—can be dated to after the middle of the 2nd until the late 4th centuries CE. These are mostly characterized by a dark weathering patina. Some types of bowls representing common dishes include examples with a crimped strip-handle (cat. no. 3), a high folded base-ring (cat. no. 4), a horizontal double fold in the glass wall (cat. no. 7) and a broad out-folded rim (cat. no. 8). Several other forms and types were also attested and await final publication. Fine tableware occurs only in one small fragment of a cut-decorated bowl, which is certainly imported (cat. no. 5).

The production of some vessel types ranged from the mid to Late Roman periods (mid 2nd to late 4th centuries AD) into the Early Byzantine period. This applies for instance to bottles and jugs with a thick trail below the rim (cat. no. 6) or a spiral trail around the neck (cat. no. 9). It is the same with conical goblets (cat. no. 11), double kohl tubes (cat. no. 12), cups decorated with a blue spiral trail (cat. no. 13), and mold-blown flasks or jugs with vertical ribs (cat. no. 10). Specific glass types of the Early Byzantine period are polycandelon lamps with a stemmed hollow foot (cat. no. 15) and goblet types like those with a hollow stem and a foot with tubular edge (cat. no. 16). A white weathering patina is characteristic for the glass from this period.

As with other genres of material culture in Jerash such as pottery and architecture, sometimes one cannot determine whether a glass object has its origin in a Byzantine or in an Umayyad workshop because no differences in material and shape are discernable. Such difficulties relate to goblets such as those with a solid stem and a solid foot (cat. no. 17) and those with a solid foot and a solid stem with one knob (cat. no. 18) as well as to polycandelon lamps with solid knobbed stems (cat. no. 19). This suggests a continuous production of local Byzantine glassmakers under the new Islamic rulers.

Without a diagnostic context, it is impossible to verify the date of three loose glass tesserae (cat. no. 20) whose associated mosaic formations are lost. Cast window panes, also represented in the finds from the Northwest Quarter (cat. no. 21), were used in Jerash throughout the periods from Mid-Roman times into the Early Islamic period.

3 | METHODS

In preparation for electron microprobe (EMP) and laser ablation (LA-)ICP-MS analyses, carefully selected fresh glass was mounted in epoxy and polished.

Major element analyses using natural mineral and glass standards were performed using the Cameca SX-100 electron microprobe equipped with five wavelength dispersive spectrometers (WDS) at the Department of Earth and Planetary Sciences, UCDavis. Quantitative WDS analysis used an acceleration voltage of 15 kV, a beam current of 10 nA and 10 μm raster lengths. Sodium loss was minimized by counting this element first on the LTAP crystal for 10 s. Similar beam condition and count times were used for analysis of the natural volcanic glass standard used for calibration of Si, Na, Fe, and Al and we found reproducibility within 2-sigma error of the reported standard values. Corning glass standard B was analyzed to monitor precision and accuracy (Brill, 1999). The given results for Corning B reproduced better than 20% for element oxide concentrations in the 0.1–0.5 wt% range (SO_2, TiO_2) and better than 9% for element concentrations above 0.5 wt% (Table 1). Analyses for samples are reported in Table 2 as averages of three repeats. Detection limits are ≈300 ppm and the analytical precision ≈1–2% for the major oxides, including Na_2O from which we conclude that Na loss due to beam damage was minimal.

Trace element concentrations were determined by LA-ICP-MS using an Agilent Technologies 7500a quadrupole ICP-MS coupled to a New Wave UP-213 nm laser ablation instrument at UCDavis Interdisciplinary Center for Mass Spectrometry. The laser is equipped with a SuperCell sample chamber that uses He as carrier gas. Data are reported as the mean of six analyses at 70% energy, 80 μm spot size, 10 Hz pulse frequency and 60 sec data acquisition time. Data reduction was done offline in Microsoft Excel using GSE-G1 as calibration standard by matching the Si counts for samples and standards to the SiO_2 concentrations determined independently from EMP analyses. Repeated analysis of GSD-1G and Corning glass B was within 3–5% of known values for most elements (Table 3).

Sr isotopic analyses. Approximately 50 mg fresh glass was dissolved in concentrated HNO_3 and HF (1:10) and Sr purified by loading the solutions onto columns with Sr-spec resin from EichromTM. Matrix, Rb, Ba, and Pb removal was achieved rinsing with 3N HNO_3 followed by elution of Sr with 0.5N HNO_3. The procedure was repeated to ensure complete separation of Sr from Rb. All reagents (HCl, HNO_3, HF) were doubly distilled or Optima grade. Isotopic analysis was done on a Nu Plasma HR MC-ICP-MS (Nu032) coupled to a DSN-100 desolvating nebulizer at UCDavis Interdisciplinary Center for Mass Spectrometry. Mass fractionation on $^{87}Sr/^{86}Sr$ ratios were corrected to $^{86}Sr/^{88}Sr = 0.1194$ and interferences of ^{87}Rb on ^{87}Sr and ^{86}Kr on ^{86}Sr were monitored by measuring signal on masses 87 (= ^{87}Rb) and 84 (= $^{84}Kr+^{84}Sr$), respectively. These signals were less than a few mV. The

TABLE 2 Summary of sample information and compositions of Jerash glasses by electron microprobe[a]

Cat. No.	Sample	Color	Typological Dating	Glass group	SiO_2	Na_2O	K_2O	CaO	Al_2O_3	FeO	MnO	MgO	P_2O_5	TiO_2	Cl	SO_2	Total
Hellenistic type																	
1	Bowl rim	Amber, translucent	2–1st BCE	Hellenistic	67.81 (9)	18.92 (29)	0.55 (2)	8.48 (13)	2.57 (18)	0.25 (5)	–	0.52 (6)	0.10 (3)	0.05 (3)	0.96 (5)	0.30 (3)	100.6
2	Bowl rim	Purple, translucent	2–1st BCE	Hellenistic	68.29 (26)	16.71 (50)	0.68 (6)	7.75 (15)	2.70 (18)	0.51 (8)	1.93 (10)	0.74 (7)	0.09 (2)	0.09 (4)	0.95 (3)	0.16 (2)	100.6
2 *R*	Bowl rim	Purple, translucent	2–1st BCE	Hellenistic	68.26 (100)	16.75 (24)	0.68 (3)	7.89 (14)	2.72 (17)	0.50 (6)	1.97 (7)	0.76 (4)	0.09 (2)	0.08 (4)	0.95 (4)	0.14 (4)	100.9
Roman type																	
5	Bowl wall	Colorless, transparent	3–4th CE	Roman Sb	71.64 (87)	18.76 (95)	0.33 (5)	4.86 (13)	1.89 (13)	0.28 (3)	–	0.48 (3)	0.03 (3)	0.07 (2)	1.18 (3)	0.22 (3)	99.8
3	Bowl rim	Light greenish blue, transparent	2–4th CE	Roman Mn	67.71 (122)	18.25 (15)	0.73 (7)	7.97 (14)	2.64 (28)	0.36 (7)	1.57 (4)	0.60 (3)	0.12 (2)	0.06 (2)	0.87 (8)	0.27 (6)	100.7
4	Bowl foot	Yellowish green, translucent	3–4th CE	Roman Sb, Mn	69.49 (95)	18.11 (96)	0.59 (3)	6.83 (19)	2.14 (9)	0.41 (3)	0.52 (14)	0.51 (5)	0.12 (2)	0.08 (2)	0.97 (5)	0.17 (6)	100.0
4 *R*	Bowl foot	Yellowish green, translucent	3–4th CE	Roman Sb, Mn	69.05 (43)	18.56 (16)	0.61 (4)	7.02 (6)	2.20 (9)	0.42 (6)	0.52 (5)	0.53 (3)	0.12 (3)	0.08 (3)	1.01 (2)	0.18 (4)	100.3
Apollonia type																	
19	Lamp	Greenish blue, translucent	6–9th CE	Apollonia	71.81 (14)	15.2 (41)	0.50 (2)	8.38 (6)	3.27 (19)	0.31 (2)	–	0.48 (4)	0.05 (2)	0.08 (1)	0.87 (6)	0.06 (2)	101.1
18	Goblet	Greenish blue, translucent	5–7th CE	Apollonia	71.40 (56)	15.00 (4)	0.54 (4)	8.97 (34)	3.07 (10)	0.40 (3)	–	0.50 (3)	0.11 (4)	0.07 (1)	0.82 (4)	0.07 (2)	101.0
17	Goblet foot	Yellowish green, translucent	5–7th CE	Apollonia	70.83 (10)	15.34 (31)	0.64 (10)	9.06 (35)	3.03 (6)	0.42 (4)	–	0.54 (3)	0.12 (3)	0.06 (2)	0.90 (10)	0.06 (4)	101.0
8	Bowl rim	Pale green, transparent	4th CE	Apollonia	72.79 (58)	13.21 (28)	0.75 (3)	8.97 (14)	3.01 (7)	0.42 (5)	–	0.56 (3)	0.13 (3)	0.07 (2)	0.83 (3)	0.03 (2)	100.8
10	Flask	Pale greenish blue, transparent	4–5th CE	Apollonia	71.27 (74)	15.26 (42)	0.77 (3)	8.26 (59)	2.96 (9)	0.45 (7)	–	0.68 (7)	0.09 (2)	0.08 (2)	0.89 (8)	0.09 (2)	100.8
20	Tesserae	Pale blue, translucent	3–9th CE	Apollonia	72.12 (20)	14.23 (49)	0.81 (4)	8.79 (9)	2.97 (13)	0.42 (6)	–	0.55 (2)	0.13 (4)	0.09 (2)	0.85 (5)	0.05 (2)	101.1
15	Lamp foot	Yellow-green, translucent	5–6th CE	Apollonia	71.25 (89)	14.22 (27)	1.00 (7)	9.25 (13)	3.08 (21)	0.48 (5)	0.06 (1)	0.59 (3)	0.12 (4)	0.08 (2)	0.69 (3)	0.08 (2)	100.9
13	Cup rim	Colorless, transparent	4–7th CE	Apollonia	70.15 (18)	15.60 (32)	1.01 (4)	8.49 (32)	3.13 (28)	0.48 (8)	–	0.59 (2)	0.15 (2)	0.09 (3)	0.67 (2)	0.14 (3)	100.6
9	Jug rim	Pale greenish blue, translucent	4–5th CE	Apollonia	67.90 (21)	14.49 (33)	1.09 (8)	9.94 (15)	3.25 (5)	0.97 (7)	0.04 (1)	0.73 (5)	0.18 (4)	0.09 (1)	0.72 (5)	0.07 (5)	99.5
21	Window	Yellowish green, translucent	4–8th CE	Apollonia	70.54 (26)	14.84 (33)	1.12 (4)	9.17 (21)	3.16 (2)	0.45 (5)	–	0.59 (2)	0.20 (8)	0.08 (3)	0.69 (3)	0.08 (4)	101.0

(Continues)

TABLE 2 (Continued)

Cat. No.	Sample	Color	Typological Dating	Glass group	SiO_2	Na_2O	K_2O	CaO	Al_2O_3	FeO	MnO	MgO	P_2O_5	TiO_2	Cl	SO_2	Total
12	Tube base	Yellowish green, translucent	4–7th CE	Apollonia	70.28 (91)	14.98 (27)	1.21 (13)	8.94 (44)	3.05 (14)	0.52 (9)	–	0.75 (3)	0.18 (4)	0.10 (2)	0.66 (7)	0.08 (3)	100.8
Apollonia Mn type																	
11a	Goblet foot	Pale olive green, translucent	4–7th CE	Apollonia low Mn	69.96 (52)	14.6 (22)	1.21 (5)	9.56 (23)	2.99 (25)	0.52 (12)	0.06 (4)	0.84 (4)	0.20 (6)	0.10 (2)	0.76 (2)	0.05 (2)	100.9
11b	Goblet foot	Pale olive green, translucent	4–7th CE	Apollonia low Mn	69.72 (28)	14.74 (25)	1.21 (6)	9.68 (32)	3.03 (3)	0.53 (9)	–	0.89 (3)	0.19 (2)	0.09 (2)	0.75 (5)	0.04 (5)	101.0
16	Goblet foot	Pale greenish blue, transparent	5–7th CE	Apollonia low Mn	70.20 (25)	16.10 (73)	0.82 (4)	8.53 (21)	2.85 (7)	0.52 (6)	–	0.69 (2)	0.12 (4)	0.10 (5)	0.79 (6)	0.11 (2)	100.9
7	Bowl rim	Pale green	4th CE	Apollonia high Mn	68.42 (48)	16.43 (56)	0.98 (5)	9.01 (19)	2.67 (7)	0.53 (3)	0.93 (5)	0.65 (6)	0.13 (4)	0.08 (2)	0.79 (3)	0.13 (2)	100.8
6	Jug rim	Pale greenish blue, transparent	3–5th CE	Apollonia high Mn	69.72 (66)	15.68 (25)	0.53 (4)	8.95 (49)	2.87 (11)	0.46 (5)	0.67 (17)	0.79 (2)	0.10 (2)	0.10 (3)	0.79 (2)	0.17 (3)	100.9
14	Plate foot	Yellowish green, translucent	5–6th CE	Apollonia high Mn	68.50 (10)	15.51 (24)	1.33 (6)	10.00 (8)	3.07 (4)	0.49 (4)	0.31 (7)	0.65 (1)	0.15 (2)	0.07 (2)	0.69 (2)	0.07 (6)	100.9

[a]Compositions are averages of three analyses per sample, except those marked "*R*" representing averages of 10 analyses obtained in a later analytical session. Values in parentheses are two standard deviations of the mean corresponding to the trailing digits. "–" indicates below detection.

TABLE 3 Elemental abundances (in parts per million) for Corning B and USGS GSD-1G glass standards determined by LA-ICP-MS in this study compared to recommended values

	Li	B	Mg	Sc	Ti	V	Cr	Mn	Fe	Co	Ni	Cu	Zn	As	Rb	Sr	Zr	Nb	Sn	Sb	Ba	Ce	Pb	Th	U
Conning B																									
Measured[a]	10.7	92.1	6207	1.72	587	190	63	1822	2179	326	716	22115	1616	14	11	146	177	0.17	166	3698	663	0.16	4502	0.81	0.22
Recommended[b]	16	112	5960	N/A	595	190	66	1870	2200	340	735	22500	1695	N/A	9	140	170	N/A	190	3500	690	N/A	4610	N/A	N/A
Relative difference[c]	31%	18%	−4%		1%	0%	4%	3%	1%	4%	3%	2%	5%		−21%	−4%	−4%		13%	−6%	4%		2%		
USGS GSD-1G																									
Measured[d]	42.4	51.2	21379	50.5	7874	43.2	43.1	227	105350	41.3	58.4	41.0	54.2	27.6	38.5	68.3	40.7	39.7	27.6	42.9	68.0	39.5	48.3	39.8	39.9
Recommended[e]	43	50	21700	52	7430	44	42	220	103400	40	58	42	54	27	37	69	42	42	29	43	67	41	50	41	41
Relative difference[c]	1%	−2%	1%	3%	−6%	2%	−3%	−3%	−2%	−3%	−1%	2%	0%	−2%	−3%	2%	3%	5%	5%	0%	−1%	5%	3%	3%	3%

[a]Averages of 10 analyses during multiple analytical sessions.
[b]Recommended values from Adlington (2017), Brill (1999), Vicenzi, Eggins, Logan, and Wysoczanski (2002), and Wagner, Nowak, Bulska, Hametner, and Günther (2012).
[c]Ratio of (recommended−measured)/recommended values times 100.
[d]Averages of 15 analyses during multiple analytical sessions.
[e]Recommended values from GeoRem database (https://georem.mpch-mainz.gwdg.de).

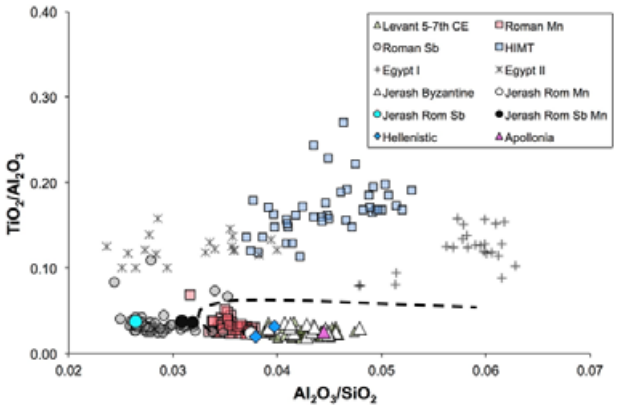

FIGURE 4 Oxide ratio variation diagram of TiO_2/Al_2O_3 versus Al_2O_3/SiO_2 for Jerash Apollonia-type samples compared to major glass groups in the 1st millennium CE. Oxides are in wt% listed in Table 2. Data sources for comparative groups: HIMT (Group 1 of Foy, Picon, Vichy, & Thirion-Merle, 2003), Apollonia (primary glass from Phelps et al., 2016; in their Table 2), Rom Mn and Rom Sb (Silvestri, 2008; Silvestri et al., 2008), Egypt I and II (Gratuze & Barrandon, 1990). Plot lay-out originally from Schibille et al. (2017) and the location of the dashed line from Freestone (in press). Groups below dashed line describe glass believed to have been made from sands at production sites along the Levantine coast (Figure 1) [Color figure can be viewed at wileyonlinelibrary.com]

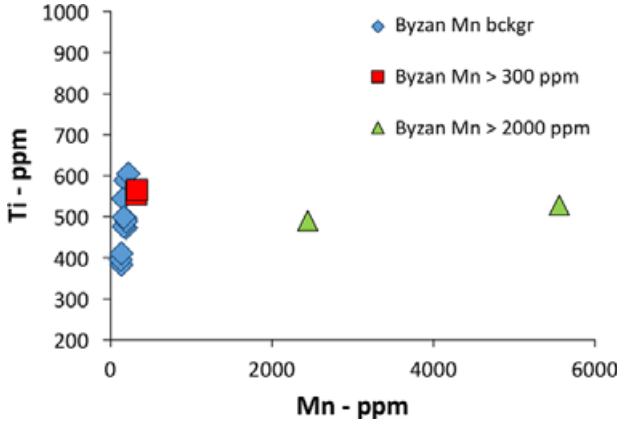

FIGURE 5 Variation diagram of Mn (ppm) and Ti (ppm) for the three groups of Byzantine glass we observe in Jerash (Table 4); Apollonia-type glass with Mn below background level (= Byzantine Mn bckgr), with low Mn (= Byzantine Mn > 300 ppm) and with high Mn contents (= Byzantine Mn > 2000 ppm) [Color figure can be viewed at wileyonlinelibrary.com]

SRM 987 standard was run after every four samples and the $^{87}Sr/^{86}Sr$ ratios of the samples normalized to an accepted value of 0.710248 for SRM 987. Normalized $^{87}Sr/^{86}Sr$ ratios of 0.705041 (± 0.000013) were obtained for standards USGS standards BCR-2. This value is within uncertainty of $^{87}Sr/^{86}Sr$ value for BCR-2 of 0.705020 ± 0.000016 (Weis et al., 2006).

4 | RESULTS

All samples classify as low-magnesium, low-potassium (<1.5 wt% each of MgO and K_2O) natron glasses (Lilyquist, Brill, & Wypyski, 1993; Sayre & Smith, 1961). Figure 4 compares the TiO_2/Al_2O_3 versus Al_2O_3/SiO_2 ratios, which may be used to distinguish the main natron glass groups occurring in the Levant around the 1st millennium CE (Freestone, Degryse, Lankton, Gratuze, & Schneider, 2018; Freestone, in press; Schibille, Sterrett-Krause, & Freestone, 2017). All of the samples plot in the area at the base of the diagram, characteristic of Roman and Byzantine period glass and especially glass made using sands of the Levantine coast. Based on this and other geochemical characteristics, 17 of the 22 glass fragments analyzed in this study classify as Byzantine glasses of the Levantine type (6 of these with Mn above 300 ppm and therefore presented separately). The remaining samples include three Roman glasses decolored by addition of antimony and/or manganese (1 Sb Roman, 1 Mn–Sb Roman, 1 Mn Roman) and two glasses from the Hellenistic period.

The manganese contents of raw glass from glass production sites in the Levant are below 250 ppm (Phelps, Freestone, Gorin-Rosen, & Gratuze, 2016). This and other studies define a threshold for the natural background level of Mn in glass from the Levant around 250 ppm (Al-Bashaireh, Al-Mustafa, Freestone, & Al-Housan, 2016; Brems & Degryse, 2014). Scatter plots of Mn versus other transition metals for the Jerash samples, show a strong correlation below 250 ppm, but samples with Mn above this value show a marked departure from the trend (e.g., Figure 5). This is important for distinguishing between the different glass groups observed in our study.

The three glasses which are typologically Roman are natron-based with CaO and Al_2O_3 contents below 8 wt% and 2.8 wt%, respectively, and Na_2O concentrations above 17 wt% (Table 2), consistent with Roman glass produced in the first centuries CE (Jackson, 2005).

Three distinct types of Roman glass are recognized primarily on the basis of their contents of the decolorizers Mn and Sb (Table 4).

1. A colorless bowl (cat. no. 5) classifies as antimony colorless Roman glass ("Rom-Sb" of Schibille et al., 2017, "Sb" of Jackson & Paynter, 2016) based on its high Sb concentration (5841 ppm) and Mn below the background level (126 ppm). The relatively low CaO and Al_2O_3 contents are characteristic of Rom-Sb glass (Jackson & Paynter, 2016).
2. Bowl cat. no. 3 belongs to the "Rom-Mn" (or "high-Mn") group given its Mn content (12,209 ppm) and Sb below 250 ppm (163 ppm). Despite the high Mn content which presumably was added as a decolorant, there is enough Fe^{2+} in this glass to color it light greenish-blue. The antimony content, although low, is well above the background level in raw glass (~1 ppm; e.g., Brems & Degryse, 2014) and indicates a component of old antimony de/colored glass.
3. Bowl cat. no. 4 has high contents of both Sb (4158 ppm) and Mn (3733 ppm) and classifies as "Rom Sb—Mn" Roman glass, which is considered to have formed by the mixing of Mn- and Sb-decolorized type glasses (e.g., Freestone, 2015; Jackson & Paynter, 2016; Silvestri, 2008). The yellowish green color is again the result of a relatively high Fe^{2+}/Fe^{3+} ratio and is typical of glass with a significant Mn content (Freestone, 2015; Silvestri, 2008).

TABLE 4 Minor and trace element composition (in parts per million) of Jerash glasses by LA-ICP-MS

Cat. No.	Glass Group	Li	B	Mg	Sc	Ti	V	Cr	Mn	Fe	Co	Ni	Cu	Zn	As	Rb	Sr	Zr	Nb	Sn	Sb	Ba	Ce	Pb	Th	U
Hellenistic																										
1	Hellenistic	3.11	135	3046	2.09	300	7.35	10.5	146	2343	1.06	2.83	3.25	6.39	1.31	8.56	524	41.8	1.27	0.54	0.97	221	12.5	7.13	0.88	1.58
2	Hellenistic	4.31	190	4310	2.98	509	27.1	17.7	14881	3597	12.2	23.7	29.7	31.7	1.76	7.76	637	51.5	1.54	1.61	1049	322	11.2	80.3	0.92	0.88
Roman																										
5	Roman Sb	3.43	212	2525	2.97	366	7.01	9.05	126	2352	1.09	2.66	4.20	14.1	10.0	4.71	331	45.3	1.40	0.36	5841	133	8.78	10.4	0.75	0.99
3	Roman Mn	3.09	99.3	3425	2.56	373	37.3	17.6	12209	3034	12.9	22.3	14.7	22.9	2.95	8.73	598	44.5	1.35	1.14	163	313	11.8	16.1	0.72	0.77
4	Roman Sb–Mn	3.63	157	2969	2.81	440	14.4	10.7	3733	2876	3.00	5.44	21.4	21.9	12.7	5.57	378	43.8	1.31	11.26	4158	209	9.12	100	0.83	0.97
Levantine I: Apollonia-type																										
19	Apollonia	4.01	33.7	2759	2.11	383	8.09	11.9	136	2910	1.13	3.59	2.99	7.05	0.86	7.79	427	40.3	1.57	0.35	0.12	244	12.8	3.39	0.73	0.58
18	Apollonia	3.31	39.7	2832	2.53	394	9.25	14.7	124	3430	1.32	4.76	35.8	16.2	1.21	8.43	413	41.0	1.59	2.40	0.19	231	11.7	11.8	0.77	0.67
17	Apollonia	3.60	50.2	3150	2.56	411	10.7	15.8	134	3336	1.43	5.07	28.3	14.1	1.22	7.07	428	41.3	1.55	2.26	0.19	235	12.1	13.6	0.79	0.77
8	Apollonia	3.95	59.0	3429	2.46	473	12.4	18.2	190	4023	2.34	5.19	19.9	11.7	1.59	10.2	444	45.1	1.67	2.50	0.95	241	13.6	37.6	0.87	1.03
10	Apollonia	4.15	87.0	4006	2.68	587	13.9	17.9	180	3998	1.96	4.36	5.22	9.22	1.63	10.5	461	62.9	2.00	1.37	0.42	231	14.3	17.7	0.94	0.85
20	Apollonia	3.81	67.0	4436	3.09	543	14.0	16.2	153	4275	2.75	5.58	9.93	12.5	2.29	9.19	447	50.1	1.99	0.99	0.93	223	12.5	13.3	0.78	0.73
15	Apollonia	3.96	62.9	3378	2.73	495	12.4	21.9	186	3935	5.87	6.45	47.6	14.0	2.03	11.9	428	52.4	1.79	4.26	1.06	230	13.3	52.6	0.86	0.92
13	Apollonia	4.06	63.3	3316	2.90	476	12.4	18.3	166	3575	2.09	5.23	20.3	13.2	2.01	12.2	443	54.6	1.82	2.56	1.24	240	12.8	48.2	0.91	1.02
9	Apollonia	4.20	59.4	3577	2.52	489	11.4	13.8	191	3540	2.37	4.43	14.8	8.74	1.80	10.0	462	53.5	1.86	1.30	0.69	236	13.2	26.8	0.90	0.86
21	Apollonia	4.02	70.9	3512	2.62	498	12.1	15.7	166	3689	1.76	5.15	11.2	10.3	1.79	11.6	444	52.8	1.80	1.50	0.71	253	14.3	17.8	0.92	1.04
12	Apollonia	4.71	86.1	4430	2.83	604	15.0	18.1	221	4527	6.54	6.48	27.7	12.4	2.17	12.2	415	63.0	2.22	1.51	1.66	238	14.6	73.3	1.04	1.24
	Average	*3.98*	*61.7*	*3529*	*2.64*	*487*	*12.0*	*16.6*	*168*	*3749*	*2.69*	*5.12*	*20.3*	*11.8*	*1.69*	*10.1*	*438*	*50.6*	*1.81*	*1.91*	*0.74*	*237*	*13.2*	*28.7*	*0.87*	*0.88*
	Standard Deviation	*0.4*	*17*	*563*	*0.3*	*73*	*2.0*	*2.7*	*30*	*459*	*1.8*	*0.9*	*14*	*2.7*	*0.4*	*1.8*	*16*	*8.1*	*0.2*	*1.0*	*0.5*	*8.0*	*1.0*	*22*	*0.1*	*0.2*
	RSD	*9%*	*27%*	*16%*	*10%*	*15%*	*17%*	*16%*	*18%*	*12%*	*67%*	*17%*	*67%*	*23%*	*26%*	*18%*	*4%*	*16%*	*12%*	*55%*	*66%*	*3%*	*7%*	*75%*	*10%*	*22%*
Levantine I: Apollonia Mn																										
11a	Apollonia low Mn	4.85	89.4	5345	2.88	558	13.2	16.9	319	4214	3.74	6.06	19.1	12.59	2.64	11.3	474	57.1	2.05	2.79	4.56	238	13.3	50.9	0.98	0.69
11b	Apollonia low Mn	4.11	76.0	5000	2.94	554	13.8	18.1	319	4384	3.71	6.17	19.0	13.86	2.95	11.1	460	51.4	2.02	2.69	4.97	226	13.0	47.2	0.84	0.61
16	Apollonia low Mn	4.78	93.1	5276	2.90	565	14.1	18.6	329	4429	3.98	5.95	20.5	12.99	2.98	11.8	487	58.2	2.14	2.77	4.74	244	14.0	54.0	1.05	0.80
7	Apollonia high Mn	4.27	90.2	3926	2.71	497	26.0	16.3	6783	4446	6.40	9.61	65.4	22.28	4.56	10.1	452	49.3	1.79	8.47	453	304	12.5	142	0.91	0.92
6	Apollonia high Mn	3.63	99.5	4543	2.80	527	16.7	17.6	5559	4021	7.98	8.98	15.8	14.62	1.64	7.21	509	58.4	1.92	0.64	0.60	290	13.5	7.30	0.91	0.84
14	Apollonia high Mn	4.11	60.9	3933	2.84	490	13.3	14.5	2442	3973	3.58	5.90	182	17.08	2.16	14.3	515	49.0	1.78	8.20	40.1	289	13.5	87.2	0.80	0.62

Values are the means of six separate spot analyses.

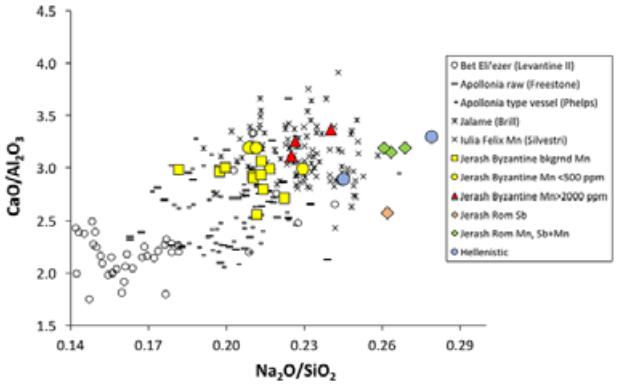

FIGURE 6 Oxide ratio variation diagram of CaO/Al_2O_3 versus Na_2O/SiO_2 for Jerash glass groups, which discriminates between Levantine primary productions of glass produced at: (1) Jalame (4th century; data of Brill, 1988, supplemented with 3rd century Rom-Mn glass from Silvestri, 2008, Silvestri et al., 2008), (2) Apollonia (6–7th century, Freestone et al., 2000, 2008, Tal et al., 2004, supplemented with vessels from Phelps et al., 2016), and (3) Bet Eli'ezer (7–8th century, Freestone et al., 2000 and unpublished). Original plot lay-out from Phelps et al. (2016). All oxides are in wt% (Table 2) [Color figure can be viewed at wileyonlinelibrary.com]

The major element compositions of the Hellenistic cast bowls (cat. nos. 1 and 2) are typical for Hellenistic glass (Reade & Privat, 2016) with Na_2O contents of 16.7 and 19 wt%, CaO from 7.8 to 8.5 wt% and Al_2O_3 from 2.5 to 2.7 wt% (Table 2) and are also closely similar to the Roman Mn and Roman Sb–Mn types. In Figure 4, they lie between the Rom Mn and Levantine I types. The purple color of cat. no. 2 is due to the presence of intentionally high MnO at around 2 wt% (e.g., Möncke, Papageorgiou, Winterstein-Beckmann, & Zacharias, 2014; Schreurs & Brill, 1984). On the other hand, cat. no. 1 has only background Mn at 146 ppm and is amber which is generally attributed to the presence of a ferri-sulfide complex (Schreurs & Brill, 1984). It may be pertinent that this glass has the highest sulfur content of those analyzed (0.3 wt%) and the absence of added manganese (Tables 2 and 4) is a typical feature of amber glass (Freestone & Stapleton, 2015; Sayre, 1963), as it is an oxidizing agent and the generation of amber requires reducing conditions.

Glass characteristic of Late Roman–Byzantine Palestine was originally defined as Levantine by Freestone et al. (2000) and this term has been heavily used in the literature. It refers to lime and alumina contents in excess of 8 wt% CaO and 2.8 wt% Al_2O_3 combined with relatively low Na_2O (<17 wt%) making them distinct from older 1st–3rd century CE Roman glass (Figure 4; Table 2; Schibille et al., 2017). Levantine glass has been divided into Levantine I type characterized by 68–71 wt% SiO_2 and 14–16 wt% Na_2O and Levantine II type with relatively higher 73–76 wt% SiO_2 and lower 11–13 wt% Na_2O contents (Freestone et al., 2000). More recently, it has been recognized that the original grouping of Levantine I incorporated the products of at least two different primary productions (Al-Bashaireh et al., 2016; Phelps et al., 2016; Schibille et al., 2017) and that these can be more-or-less separated on the basis of composition: 6th–7th century CE glass from Apollonia (Freestone, Jackson-Tal, & Tal, 2008; Tal, Jackson-Tal, & Freestone, 2004) and 4th century CE glass from Jalame (Brill, 1988). Figure 6 presents our data in terms of CaO/Al_2O_3 and Na_2O/SiO_2 ratios, which pull apart glass from the two production sites (Phelps et al., 2016) and also separate Apollonia glass from natron glass (previously Levantine II) from the Umayyad production site at Bet Eli'ezer, Hadera (Al-Bashaireh et al., 2016). The reference data for Roman period Jalame glass are supplemented with data for Rom-Mn glass from the 3rd century CE Iulia Felix wreck (Silvestri, 2008; Silvestri, Molin, & Salviulo, 2008) and for the Byzantine Apollonia-type with the analysis of vessels from Palestine (Phelps et al., 2016).

Whereas the typologically Roman and Hellenistic glasses analyzed plot on the right-hand side of Figure 6, similar to 4th century Jalame, the 14 Late Roman–Byzantine (4th century CE or later, Table 2) samples which have natural levels of Mn or low Mn levels up to 500 ppm lie to the left, plot in the Apollonia field or have compositions which straddle the boundary between Jalame and Apollonia glasses. In addition to their dating, the low manganese contents of these glasses are consistent with their assignation to Apollonia rather than Jalame since deliberately added Mn is present in about half of the glass analyzed from Jalame (Brill, 1988) whereas this has not been observed in primary glass from Apollonia tank furnaces.

Catalogue numbers 11a, 11b, 16 which have slightly elevated (≈300 ppm) Mn are separated in the analytical tables and in the figures, as they are shifted slightly towards the Jalame field (see above; Figure 6). However, the low Na_2O contents of these glasses associate them with Apollonia-type production and we consider them as Apollonia-type glass, with admixing of a small amount of older Mn-decolorized material. These are henceforth referred to as "low-Mn" as opposed to glasses with "background" levels of Mn. Cat. nos. 6, 7, and 14 have significantly elevated (> 2000 ppm) manganese and could be interpreted as Jalame-type glasses (Figure 6; Table 2). However, their intermediate soda, lime, and alumina contents coupled with elevated Sb in cat. nos. 7 and 14 (Tables 2 and 4), suggests that these may be genuinely intermediate, the result of mixing Apollonia-type glass with older decolorized types, and we group them with the other Byzantine forms as Apollonia-type glass.

None of the glasses analyzed corresponds to the field of the majority of low-soda high-silica products of the 7th–8th century CE furnaces at Bet Eli'ezer (Figure 6).

5 | DISCUSSION

5.1 | Origins of primary glass types in Jerash

The strontium isotope data indicate that most of our samples have $^{87}Sr/^{86}Sr$ ratios close to the Holocene seawater (and beach shell) value of 0.7092 (Table 5, Figure 7). However, the $^{87}Sr/^{86}Sr$ ratios of Rom-Mn cat. no. 3 (0.708489) and purple Hellenistic bowl cat. no. 2 (0.708834) are low. These two samples have the highest Mn contents in our dataset and also relatively high Sr (Figure 7), characteristics which are now recognized as likely to reflect the presence of old strontium contaminant in the manganese oxide added as decolorant (Gallo et al., 2015; Ganio et al., 2012). Accepting this, all of the samples analyzed are consistent with manufacture from coastal sands.

Figure 8 compares mean values for trace elements expected to remain undisturbed by later colorant additions for the Jerash glass

TABLE 5 Sr isotope compositions of Jerash glass by MC-ICP-MS

Cat. No.	Glass Groups	$^{87}Sr/^{86}Sr$ (2σ)[a]
Hellenistic		
1	Hellenistic	0.709130 (15)
2	Hellenistic	0.708833 (110)
Roman		
5	Roman Sb	0.708903 (15)
3	Roman Mn	0.708489 (18)
4	Rom Sb, Mn	0.708987 (14)
Levantine I: Apollonia-type		
19	Apollonia	0.709054 (15)
19*R*[b]	Apollonia	0.709070 (11)
17	Apollonia	0.708985 (11)
20	Apollonia	0.709132 (14)
13	Apollonia	0.708909 (25)
9	Apollonia	0.709032 (10)
21	Apollonia	0.708989 (16)
Levantine I: Mn		
11b	Apo low Mn	0.708902 (20)
16	Apo low Mn	0.708907 (16)
7	Apo high Mn	0.708904 (18)
6	Apo high Mn	0.708993 (13)
14	Apo high Mn	0.708987 (14)
Total procedural blank = 0.06 ng Sr		

[a]Two sigma analytical precision corresponding to the trailing digits.
[b]Repeat analysis.

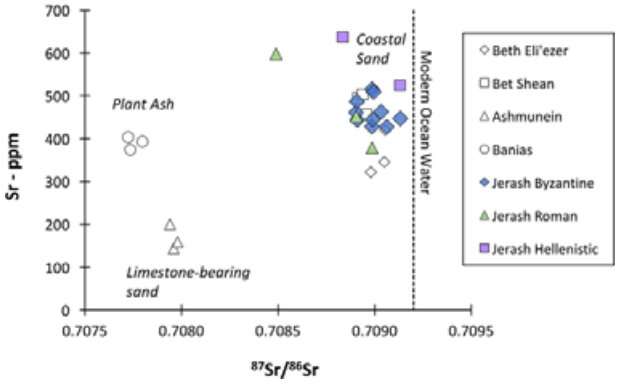

FIGURE 7 Variation plot of $^{87}Sr/^{86}Sr$ ratios (Table 5) versus strontium concentration (in ppm; Table 4) of Jerash Byzantine, Roman, and Hellenistic glass groups. Jerash Byzantine group includes glasses with background, low and high manganese concentrations. Jerash Roman group include all three Roman Sb, Roman Mn and Roman Sb–Mn glasses. Original plot lay-out from Freestone et al. (2003). The two glasses with high Sr and relatively low $^{87}Sr/^{86}Sr$ are characterized by high manganese (Hellenistic glass cat. no. 2 and Roman Mn glass cat. no. 3; Table 4). Apollonia data from Brems et al. (in press) [Color figure can be viewed at wileyonlinelibrary.com]

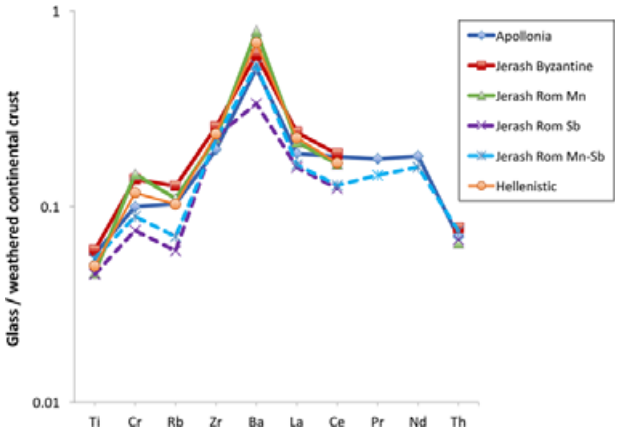

FIGURE 8 Trace element concentrations (ppm) related to the sand source in glass production for the Jerash glass groups normalized to the weathered continental crust (MUQ of Kamber et al., 2005). Our groups are compared to primary glass from Apollonia (Phelps et al., 2016). Jerash Byzantine glasses include low and high Mn groups. Note the logarithmic scale [Color figure can be viewed at wileyonlinelibrary.com]

groups and for primary glasses from Apollonia (data from Phelps et al., 2016). These fingerprint the Levantine coast as the source for the Apollonia glasses from Jerash, and show the strong similarities between the Rom-Mn, Hellenistic glasses, and primary Apollonia glass. Rom-Mn glass is generally considered to have originated on the coast of the Levant (Nenna et al., 1997), and these data are consistent with that view. The Hellenistic glasses are similar in major and trace compositions, and are likely to have originated in the same region.

In the 1st century CE, the production of antimony-decolorized glass was established and it appears to have been preferred for more expensive items such as tableware with cut decoration (Jackson & Paynter, 2016). The Roman Sb and Roman Mn–Sb glasses from Jerash differ significantly from the Byzantine, Rom-Mn, and Hellenistic glasses in terms of Rb, Ba, and LREE (La, Ce) in particular (Figure 8). This supports the view that Rom-Sb glass was not a product of Palestine and more likely originated from Egypt (Degryse, 2014; Schibille et al., 2017).

The results therefore suggest that glass used at Jerash from the Hellenistic through to the Umayyad period originated mainly from the tank furnaces of the Levantine coast, with the possible exception of antimony-decolorized Roman glass of 2nd–4th centuries CE. Glass types generally considered to have an Egyptian origin which were common in other regions in the 4th–7th centuries CE, such as Egypt I, Egypt II, HIMT, and Serie 2.1 or HLIMT (Ceglia et al., 2015; Schibille et al., 2017) are absent from the samples analyzed (Figure 4). However, this could be a sampling effect and small quantities of these types might have reached Jerash; this possibility will be further explored in later studies.

Of particular interest is that no glass which might have originated in the tank furnaces at Bet Eli'ezer (Levantine II of Freestone et al., 2000) has been detected. The Bet Eli'ezer furnaces appear to have been in production from about 670 CE (Phelps et al., 2016). The absence of this glass type in Jerash suggests that none of the glasses analyzed date later than the third quarter of the 7th century CE. This is possible, as typologically all of the forms could date to late Byzantine times or earlier. Furthermore, Bet Eli'ezer-type glass has been identified at another site in Jordan, Umm el-Jimal, located away from the coast but some

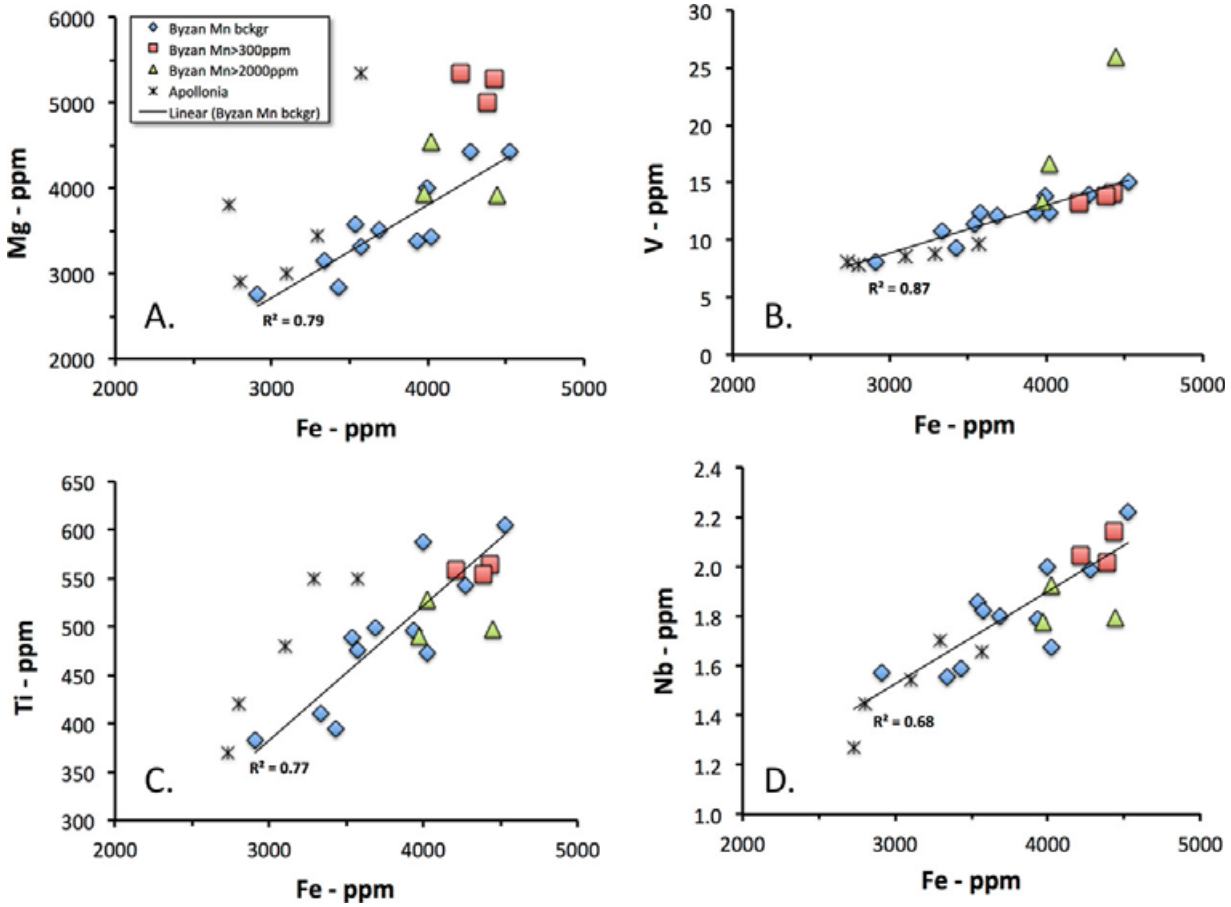

FIGURE 9 Mg versus Fe. (b) V versus Fe. (c) Ti versus Fe. (d) Nb versus Fe for Byzantine Jerash glass groups. All concentrations are in ppm (Table 4). Reported R^2 values are for fitted regression lines for the glass samples with background manganese concentrations. Data for primary glass from the furnaces at Apollonia from Phelps et al. (2016) [Color figure can be viewed at wileyonlinelibrary.com]

55 km to the North of Jerash (Al-Bashaireh et al., 2016). However, an alternative explanation might be that, in the Umayyad period (661–750 CE), fresh glass from the coast was no longer reaching Gerasa and that the glass workers were entirely dependent upon recycled material.

It is pertinent that the glass of the 2nd–4th century CE typically has a dark weathering patina, whereas the 6th–7th century CE fragments weather to an opaque white. The precipitation of manganese oxide in the weathered layers is well-known as the cause of the darkening of medieval European glass (Schalm et al., 2011) and it seems likely that this is also the case for Jerash, as the Roman-period pieces typically have high levels of MnO, whereas the later glasses typically have MnO at background levels. The Roman-period antimony-decolorized glass, cat. no. 5, has low manganese, and also weathers to an opaque white patina, consistent with these observations.

5.2 | Secondary processing phenomena: recycling in the Apollonia-type glasses

The discussion below will focus on the Apollonia-type glasses since these are by far the most dominant group in our sample-set and because they show distinct features that relate back to production and postproduction processes in secondary workshops. The location of the glass workshops which made the vessels in Jerash have yet to be determined by excavation, but it seems very likely that, like other cities in the region in Late Antiquity they were in the immediate vicinity.

A number of compositional effects might be anticipated from the mixing and remelting processes which comprise a glass recycling system: (1) mixing of different primary glass compositions, (2) contamination from the melting furnace/crucibles and iron glass working tools, (3) contamination with colorants and decolorizers from the incidental inclusion of old colored glass in the batch, (4) contamination by components of fuel and fuel ash, and (5) loss of volatile components to the furnace atmosphere. By definition, if a glass object is remelted to make a new one, then it is recycled, and evidence for remelting is therefore evidence for recycling.

In terms of mixing different glass types, we have observed above that the Byzantine glasses with high Mn lie closer to earlier Roman glasses in terms of major components such as Na_2O (Figure 6) and that this is the result of mixing Apollonia-type glass with Roman Mn-decolorized glass. No other compelling evidence of mixing of primary glasses is recognized here, but this process is implicit in some of the data, for example, the behavior of colorant-related elements, below.

There is a strong correlation between Fe and Mg in the Apollonia-type glasses from Jerash which is also present for other transition metal elements such as Ti, V, and Nb (Figure 9). An enrichment in

Fe has been observed in Roman Mn–Sb glass from York, UK and ascribed to contamination from ceramic melting pots or iron blowpipes (Jackson & Paynter, 2016). If the Fe was derived from an iron tool, departure from the trend with MgO would be expected and this does not occur (Figure 9a). Contamination from the furnace is a possibility, but the high Mg:Fe ratio of 1:1 indicates control from heavy minerals such as amphibole, pyroxene, spinel, and zircon (e.g., Molina, Scarrow, Montero, & Bea, 2009) rather than clays which are generally strongly dominated by Fe relative to Mg (e.g., Kamber, Greig, & Collerson, 2005). Therefore, the covariations in the Apollonia samples are a primary feature controlled by differences in the accessory mineral assemblage of the individual batches of coastal sand used for their production. A similar explanation has also been offered by Schibille et al. (2017) for FeO–MgO covariations in Rom-Sb glasses that they analyzed from Carthage. However, the Rom-Sb glasses reported by Schibille et al. (2017) have an MgO:FeO ratio of 2:1, relative to Mg and Fe covariation of 1:1 in the Jerash glasses (Figure 9). These very different Mg/Fe ratios support the hypothesis (see above) that the Sb-decolorized glass did not originate in the Levant, but elsewhere, possibly Egypt.

In addition to iron and other transition metal oxides, an increase in alumina concentration might be expected if a glass was significantly contaminated by furnace ceramic during remelting. Figure 6 shows no enrichment in Al_2O_3 of the Jerash samples relative to Apollonia primary glass and we can therefore assume from this and the iron oxide that contamination of the glass from ceramics (furnace) during any recycling that occurred was minimal. This differs from the conclusions of Jackson and Paynter (2016) and may reflect the arrangement of the furnace. In the Levantine region, there is limited evidence for the use of pots or crucibles in which glass was melted and it appears that even at the secondary stage, the glass was melted in tanks (e.g., Gorin-Rosen, 2000); this was also the case in larger centers in the West, for example Roman London (Wardle, 2015). There is evidence, however, for melting pots at York, UK studied by Jackson and Paynter (op. cit.). Tanks will typically have had a much larger volume to surface area ratio than pots or crucibles and the interaction between the walls of the tank bulk of the glass will have been correspondingly less, explaining the discrepancy.

A distinctive group of elements, including Cu, Sn, Pb, Co and Sb, shows different behavior. Figure 10 shows that where crustal values are available (Kamber et al., 2005), these elements show a substantially higher level of enrichment in our glasses than those elements associated with accessory minerals. They are the elements associated with glass coloration and, following earlier studies (Freestone, Ponting, & Hughes, 2002; Jackson, 1996; Mirti, Lepora, & Saguì, 2000), it is considered that a significant component originates in the incidental incorporation of small amounts of earlier colored glasses in recycling processes. This effect of recycling on the distributions of these elements is conveniently illustrated in terms of the coefficients of variation (relative standard deviations) for the individual elements (Figure 11). The colorant elements have very high CVs due to the imperfect nature of the recycling process and the failure to completely mix and homogenize separate glass batches. Furthermore, several element pairs show very strong correlations, such as Cu–Sn, and Pb–Sb

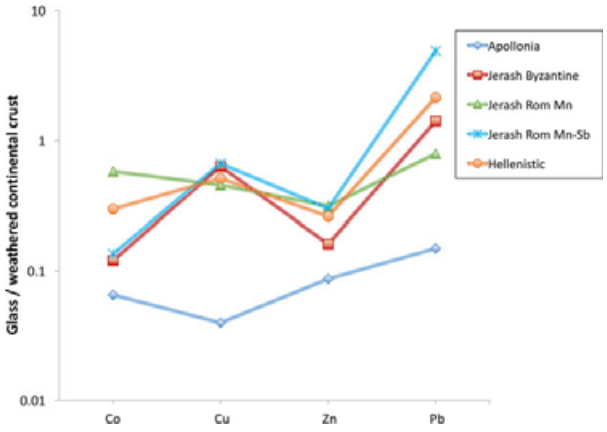

FIGURE 10 Trace element concentrations (ppm) related to colorants addition to glasses normalized to weathered continental crust (MUQ of Kamber et al., 2005). Our groups are compared to primary glass composition from Apollonia (Phelps et al., 2016). Jerash Byzantine glasses include low and high Mn groups. Note the logarithmic scale [Color figure can be viewed at wileyonlinelibrary.com]

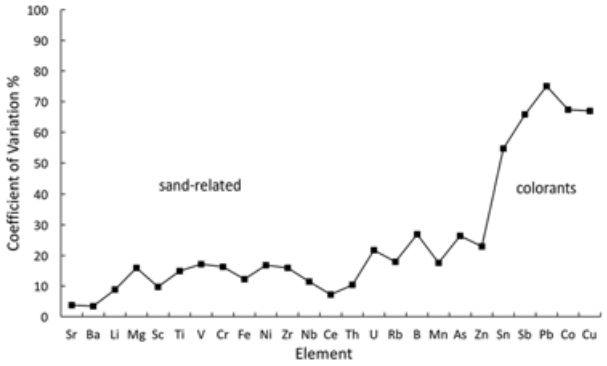

FIGURE 11 Coefficients of variation (= relative standard deviations) for trace elements in for all Apollonia-type glasses with background levels of Mn (Table 2). Sand-related elements typically have low CVs whereas those associated with colorants are high. Elements associated with alkali and ash—U, Rb, and B are intermediate

(R^2 of 0.75 and 0.81, respectively), and these appear to reflect specific coloring agents such as bronze scale and lead antimonate. The implication is that, whereas the Apollonia-type glasses from Jerash show features fully consistent with a single primary production, there has been significant recycling and this is reflected in the colorants. Furthermore, analysis of glass from tank furnaces on the Levantine coast indicates Pb values typically less than 10 ppm, and Cu values less than 5 ppm (Brems et al., in press; Phelps et al., 2016), whereas with only one exception, our Apollonia-type glasses contain higher levels (Table 4) suggesting that the great majority of the Apollonia-type glass analyzed here contains some recycled material.

5.3 | Influence from fuel and furnaces during recycling in Jerash

Evidence that the Apollonia-type glasses had been through one or more episodes of recycling has been inferred above from the colorant element concentrations. The effects of workshop practices on glass composition have been explored experimentally by Paynter (2008)

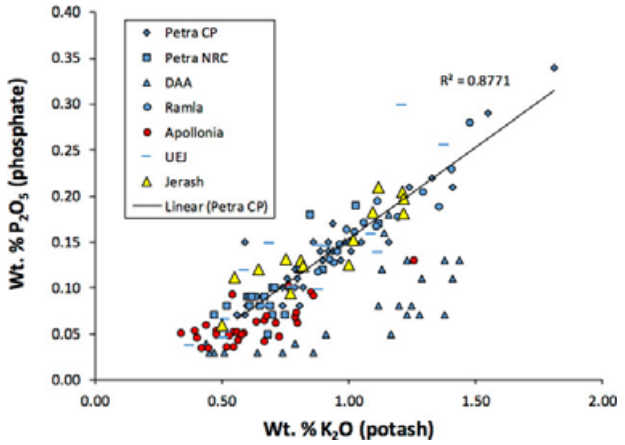

FIGURE 12 Oxide variation diagram of P_2O_5 versus K_2O in wt% (representing contamination from fuel ash) for Jerash Byzantine glass groups with background and low Mn compared to Byzantine glass compositions observed at other Levant cities. Data for Petra, Deir Ain Abata (Rehren et al., 2010), Ramla, Israel (Tal et al., 2008), and Umm el-Jimal, Jordan (Al-Bashaireh et al., 2016). Primary glass from Apollonia from Phelps et al. (2016). R^2 value is for fitted regression line through Jerash glass group [Color figure can be viewed at wileyonlinelibrary.com]

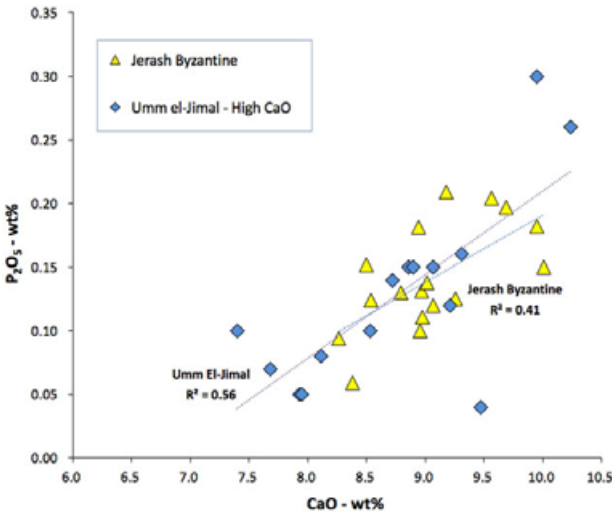

FIGURE 13 Oxide variation diagram of wt% CaO versus P_2O_5 for "High CaO"-group of Byzantine samples observed at Umm el-Jimal (Al-Bashaireh et al., 2016) compared to the Byzantine samples in this study; this group includes samples with background Mn and low Mn. The R^2 value is for fitted regression line for this group [Color figure can be viewed at wileyonlinelibrary.com]

who showed that in addition to accumulation of Al and Fe from the melting pot, remelting of Roman-type soda lime glasses in reconstructed Roman glass furnaces subjects the glass to contamination by K from fuel ashes and/or vapors. While we can expect the contaminants to have been strongly controlled by the type of glass, the fuel, the firing temperatures and the type of clays used to make the furnace, Paynter's study provide some important clues about potential influences from furnace and fuel.

Concentrations of K_2O and P_2O_5 in Levantine I glasses from Jerash are high, up to 1.33 and 0.21%, respectively. Not only are these values twice as high as in glass from the primary furnaces at Apollonia (Freestone et al., 2000; Tal et al., 2004), but these two components are strongly correlated (R^2 of 0.88 in Figure 12). The K_2O and P_2O_5 correlation observed for the Jerash glasses is most likely the result of interaction with the fuel ash and fuel ash vapors during remelting and/or working as has been observed for Apollonia-type glass at other contemporary sites such as Petra, Jordan (Rehren, Marii, Schibille, Stanford, & Swan, 2010), Ramla, Israel (Tal, Jackson-Tal, and Freestone (2008) and Umm el-Jimal, Jordan (Al-Bashaireh et al., 2016) (Figure 12). However, other components which might be affected by fuel ash contamination, particularly MgO and CaO (cf. Al-Bashaireh et al., 2016) do not appear to have been perturbed in the Jerash glass. Figure 13 shows that relative to observations for the Byzantine glass at Umm el-Jimal, Apollonia-type glass at Jerash shows a lower spread in CaO (8–10 vs. 7–10.5 wt%) and P_2O_5 (0.05–0.2 vs. 0.05–0.3 wt%) concentrations as well as lower degree of correlation (R^2 of 0.41 vs. 0.56). This may be due to the configuration of the Jerash furnace(s), so that the glass was protected from contamination by solid ash, and the contamination was largely from the vapor, but it could also be due to the type of fuel used.

A plausible fuel for Jerash is olive pits, given the finds of olive crushing mills and olive pits in many layers in Jerash. There is little doubt that olives have played a role regionally and oil production in general was significant (e.g., Ali, 2014). Rowan (2015) has drawn attention to the extensive evidence for the use of pomace, olive-pressing waste, as a fuel in antiquity. Olive pits as fuel for glass production are particularly suitable, since their fire burns hotter than wood and therefore they have excellent qualities for glass melting. Large amounts of charred olive pits were found close to glass furnaces in Beth Shean (Gorin-Rosen, 2000) and Sepphoris (Fischer & McGray, 1999), but until now evidence for the actual use of these for firing has not been drawn from the chemistry of the glass samples. Data on the chemistry of olive residues is available due to modern interest in their potential as a biofuel. These indicate 44% K_2O relative to 8% CaO for olive pit ash (Miranda, Esteban, Rojas, Montero, & Ruiz, 2008), 44% K_2O relative to 4% CaO for olive pomace (ECN Phyllis2 database for biomass and waste; https://www.ecn.nl/phyllis2/) or 28% K_2O relative to 18% CaO for the ash of "olive residue" (Gogebakan & Selçuk, 2009). It is clear that the potash to lime ratio of olive pit/residue ash is significantly higher than those of most hard and soft wood ashes, in which lime is generally in excess of potash (e.g., Misra, Ragland, & Baker, 1993). Therefore, furnaces operating with a high proportion of olive pits in the fuel would produce ash with substantially more K_2O than those firing mainly wood. The high level of enrichment of potash observed in this study and in other glasses from Jordan strongly suggests that olive pits were a significant component of the fuel used, consistent with the archaeological evidence from the region. Miranda et al. (2008) report that their olive pit ash also contained 3.43% P_2O_5, which would volatilize and explain the correlation observed between phosphate and potash.

We observe a negative correlation between potash and chlorine, which has previously been observed in glasses from Umm el-Jimal (Al-Bashaireh et al., 2016) and may also be observed in glass analyzed from Petra (Rehren et al., 2010) (Figure 14). Chlorine in the primary glass

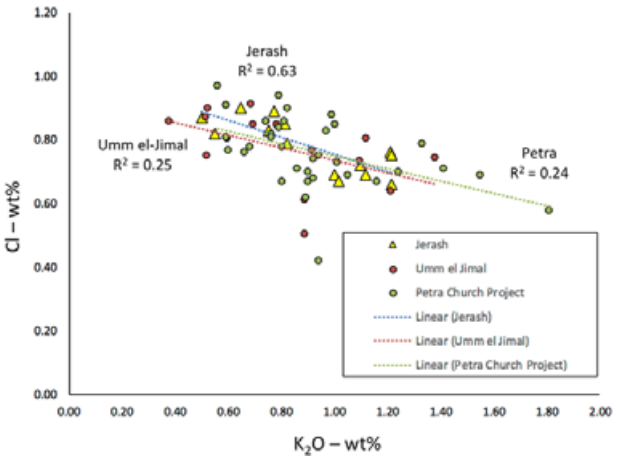

FIGURE 14 Oxide variation diagram of wt% Cl versus K_2O (fuel ash) for Levant cities. Data as in Figure 12 [Color figure can be viewed at wileyonlinelibrary.com]

originates from the natron and would normally be expected to show a positive correlation with soda (Na), also coming from the natron, and be stabilized in the melt due to sodium–chloride (Dalou, Le Losq, Mysen, & Cody, 2015). However, given the volatile nature of chlorine, as well as the alkalis, repeated melting, particularly at high temperature, inevitably leads to Cl (and to a lesser degree alkali) loss (Freestone & Stapleton, 2015). This does not explain the antithetical relationship seen for Cl and K in Jerash Byzantine glass (Figure 14). As for Umm el-Jimal and Petra, we ascribe this correlation to a combination of recycling (leading to chlorine loss) and contamination by fuel ash (leading to increased potassium). Moreover, the strong negative K–Cl correlation ($R^2 = 0.63$) compared to other sites in the region (Umm el-Jimal at 0.25 and Petra at 0.24), in addition to even stronger positive K–P correlation ($R^2 = 0.88$; Figure 12), suggests that glass recycling was more intensive at Jerash.

Jackson, Paynter, Nenna, and Degryse (2016) have recently suggested that a negative correlation between CaO and Cl among Roman glass groups and experimental glass synthesized using Egyptian natron is a signature of primary glass production. The lack of a similar correlation among the Byzantine glasses of Jerash ($R^2 = 0.2$) does not exclude this possibility, but does suggest that additional factors affect Cl and Ca in Levantine glasses. Based on our current understanding of chlorine solubility in silicate melts, chlorine is expected to increase with the abundance of network-modifiers (e.g., monovalent and divalent cations (Na^+, K^+, Ca^{2+}, Mg^{2+}, Mn^{2+}, Fe^{2+}, etc.) in excess of those needed to locally charge balance Al^{3+} (Carroll, 2005; Metrich & Rutherford, 1992; Veksler et al., 2012). This expectation is realized for medieval and postmedieval glasses where Na and Cl are positively correlated (Schalm, Janssens, Wouters, & Caluwé, 2007; Wedepohl, 2003) and supported by evidence of immiscible droplets of sodium chloride in ancient Cl-rich glass soda lime–silica glasses (Barber & Freestone, 1990; Barber, Freestone, & Moulding, 2009). Finally, the importance of alkali–Cl complexes in the melt and inevitability of Cl loss during fusion are corroborated by the relatively high chlorine contents of Roman amber glass which have been suggested to be the result of relatively short melting durations used to preserve the color (Freestone & Stapleton, 2015). In conclusion, our observation that chlorine abundance is antithetical to potash for Jerash Byzantine glass and the lack of demonstrable correlations with soda and lime is consistent with recycling, and thus not a feature of primary glass production. We are not proposing that Cl abundance is a universal tracer of recycling, melting duration or melting temperature, but rather, when one considers glasses of similar major element composition from similar technological context, chlorine content coupled with correlations (or not) with other glass constituents is a useful indicator of recycling.

5.4 | Compositional dependence upon the context of the glass recycling economy

The Jerash data emphasize the complexity of the glass recycling process and the dependence of the composition of the recycled glass upon the local social context. It has been observed that the characteristics of recycling differ from those in some western contexts, such as York, as contamination from container ceramics is not apparent. Furthermore, the elevated values and strong correlations for potash and phosphorus observed here are not as apparent in western Roman glasses which are believed to have been recycled (e.g., Freestone, 2015; Silvestri, 2008) or even in Apollonia-type glass from Israel (Phelps et al., 2016) and this may be related to the fuel used.

It is also noted that in Umm el-Jimal, in northern Jordan, Apollonia-type glasses show a greater overall enrichment in trace metals generally added as colorants, where Cu and Pb enrichments are detectable using EPMA rather than the trace levels observed here (Al-Bashaireh et al., 2016). This is likely to stem from the nature of the reservoir of glass undergoing recycling. The Umm el-Jimal glass was recovered from churches where storage of colored glasses from mosaics for recycling might be expected, as has been observed at Petra (Marii & Rehren, 2009). We speculate that this led to relatively high contents of glass colorants in the glass from Umm el-Jimal. The glass from Jerash analyzed here originates from domestic houses, shows relatively weak enrichment in colorant elements but strong evidence of recycling in the fuel-related components.

There is substantial archaeological evidence from Jerash which attests to the collection of glass possibly for recycling. Such glass heaps stem from the churches and especially from the passage north of St. Theodore and from a room under the north stairs from the Fountain Court (Baur, 1938 in: Kraeling 514–515). Also, evidence for already recycled material in the form of glass cakes probably prepared for the production of glass tesserae has been found in Jerash in the so-called Glass Court (Baur, 1938 in: Kraeling 517–518). Future work, comparing glass associated with the churches with that from more secular, domestic contexts, might cast light on the organization of the glass industry in the Levant at this time.

6 | CONCLUSIONS

The excavated glass from Jerash, Jordan, dating to between the Hellenistic and the Late Byzantine periods, derives mainly from the Levantine coast with some, possibly Egyptian, antimony-decolorized glass

in the Roman period. The Byzantine glass, which dominates the assemblage, derives mainly from the tank furnaces located in or around Apollonia. A consideration of the manganese contents of the Apollonia-type glass indicates that it is generally present at background levels, and where present is the result of remelting and mixing of Roman glass during recycling.

Significant evidence for recycling is observed in the form of elevated potash and phosphate contamination from the fuel, as well as elevated transition metals. Concomitantly, there was a depletion in chlorine, due to volatilization at high temperature. For the first time, we draw attention to the effect of recycling on the coefficients of variation of trace elements in the glass. These types of indicator can provide clues as to the relative intensity of the recycling process, which elemental concentrations alone do not.

Despite the apparent proximity of Jerash to primary glass production sites near the Levantine coast, an efficient system for recycling of old glass must have been in place. The implication of a well-organized recycling system in Jerash suggests limited glass import from the Levantine coast and elsewhere, which is supported by the finds of only few Roman glasses and a lack of Egyptian-type glasses. The localized nature of recycling in Jerash displays important regional differences, which we relate to differences in interaction zones and proximity to the production sites at the Mediterranean coast.

The characteristic K-enrichment observed at Jerash and other Levantine locations has implications for the type of fuel used and is likely to indicate a significant component of olive-pressing residue. Differences between Jerash and other sites in the region such as Umm el-Jimal suggest that the nature and degree of over-printing of primary compositions by secondary recycling processes are specific to the context within which the recycling took place. Technological factors relating to local practice, as well as the types and quantities of glass available for recycling, may provide a fingerprint of the secondary workshop. In favorable circumstances, this may allow the attribution of glass vessels to secondary workshops through elemental analysis. The phenomenon of recycling fits well to the overall economic situation of the cities in the region of the 7th–8th centuries CE. The towns underwent a considerable process of on the one hand urban industrialization and on the other localization of trade networks (see e.g., Avni, 2014, 290–294; Walmsley, 2000, 305–309; 321–329; 335–337). Both processes are apparent in recycling which attests to local production within the city and limited supply of (or high demand for) raw materials.

ACKNOWLEDGMENTS

We would like to acknowledge the generous funding received for the undertaking of the Danish–German Jerash Northwest Quarter Project since 2011 from The Carlsberg Foundation, The Danish National Research Foundation (grant number 119), Deutsche Forschungsgemeinschaft, Deutsche Palästina-Verein, EliteForsk Award, and H. P. Hjerl Hansens Mindefondet for Dansk Palæstinaforskning. Furthermore, we thank Greg Baxter at the UCDavis thin section lab, Sarah Roeske at the UCDavis microprobe lab and Justin Glessner at the UCD Interdisciplinary Center for Mass Spectrometry. We thank Stephen Koob at the Corning Museum of Glass for providing us with Corning glass standards. GHB acknowledges support by the Danish National Research Foundation for the Niels Bohr Professorship at Aarhus University. We thank Charles Lesher, two anonymous reviewers, and the associate editor for providing constructive comments that significantly improved this paper.

ORCID

Gry Hoffmann Barfod http://orcid.org/0000-0002-7000-0757
Ian C. Freestone http://orcid.org/0000-0002-8223-4649
Achim Lichtenberger http://orcid.org/0000-0003-2653-9859
Rubina Raja http://orcid.org/0000-0002-1387-874X

REFERENCES

Adlington, L. (2017). The Corning archaeological reference glasses: New values for "old" compositions. *Papers from the Institute of Archaeology*, *27*(1); Art. 2, pp. 1–8.

Adam-Veleni, P. (2010). *Glass cosmos*. Thessaloniki: Archaeological Museum of Thessaloniki.

Al-Bashaireh, K., Al-Mustafa, S., Freestone, I. C., & Al-Housan, A. Q. (2016). Composition of Byzantine glasses from Umm el-Jimal, northeast Jordan: Insights into glass origins and recycling. *Journal of Cultural Heritage*, *21*, 809–818.

Ali, N. (2014). Olive oil production in a semi-arid area: Evidence from Roman Tell Es-Sukhnah, Jordan. *Mediterranean Archaeology and Archaeometry*, *14*(2), 337–348.

Antonaras, A. (2012). *Fire and sand: Ancient glass in the Princeton University Art Museum*. New Haven: Yale University Press.

Arinat, M., Shiyyab, A., & Abd-Allah, R. (2014). Byzantine glass mosaics excavated from the Cross Church, Jerash, Jordan: An archaeometrical investigation. *Mediterranean Archaeology and Archaeometry*, *14*(2), 43–53.

Arveiller-Dulong, V., & Nenna, M. -D. (2005). Les verres antiques du Musée du Louvre II, Paris. *Topoi*, *15*(2), 775–786.

Atik, S. (2009). Late Roman/Early Byzantine glass from the Marmaray rescue excavations at Yenikapi. In E. Laflı (Ed.), *Istanbul, in Late Antiquity/Early Byzantine glass in the eastern Mediterranean* (pp. 1–16). Izmir: Tübitak.

Avni, G. (2014). *The Byzantine-Islamic transition in Palestine: An archaeological approach*. Oxford: Oxford University Press.

Barber, D. J., & Freestone, I. C. (1990). An investigation of the origin of the colour of the Lycurgus Cup by analytical transmission electron microscopy. *Archaeometry*, *32*(1), 33–45.

Barber, D. J., Freestone, I. C., & Moulding, K. M. (2009). Ancient copper red glasses: Investigation and analysis by microbeam techniques. In A. J. Shortland, I. C. Freestone, & T. Rehren (Eds.), *From mine to microscope–Advances in the study of ancient technology* (pp. 115–127). Oxbow Books and the David Brown Book Company.

Baur, P. V. C. (1938). Glassware. In C. H. Kraeling (Ed.), *Gerasa. City of the Decapolis* (pp. 505–546). New Haven: ASOR.

Brems, D., & Degryse, P. (2014). Trace element analysis in provenancing Roman glass-making. *Archaeometry*, *56*, 116–136.

Brems, D., Freestone, I. C., Gorin-Rosen, Y., Scott, R., Devulder, V., Vanhaecke, F., & Degryse, P. (in press). Characterisation of Byzantine and Early Islamic primary tank furnace glass. *Journal of Archaeological Science Reports*.

Brill, R. H. (1988). Scientific investigations. In G. D. Weinberg (Ed.), *Excavations at Jalame: Site of a glass factory in late Roman Palestine* (pp. 257–294). Columbia: University of Missouri Press.

Brill, R. H. (1999). *Chemical analyses of early glass* (Vol. *1*). New York: The Corning Museum of Glass.

Çakmakçi, Z. (2009). A typological approach to glass goblet production from Late Antiquity to the Middle Ages in the light of recent finds. *Late Antiquity/Early Byzantine Glass in the Eastern Mediterranean*, *2009*, 49–66.

Carroll, M. R. (2005). Chlorine solubility in evolved alkaline magmas. *Annals of Geophysics*, *48*(4–5), 619–631.

Ceglia, A., Cosyns, P., Nys, K., Terryn, H., Thienpont, H., & Meulebroeck, W. (2015). Late antique glass distribution and consumption in Cyprus: A chemical study. *Journal of Archaeological Science*, *61*, 213–222.

Czurda-Ruth, B. (2007). Hanghaus 1 in Ephesos. Die Gläser, Forschungen in Ephesos. *Gnomon*, *81*, 665–667.

Dalou, C., Le Losq, C., Mysen, B. O., & Cody, G. D. (2015). Solubility and solution mechanisms of chlorine and fluorine in aluminosilicate melts at high pressure and high temperature. *American Mineralogist*, *100*(10), 2272–2283.

Degryse, P. (2014). *Glass making in the Greco-Roman world: Results of the ARCHGLASS project*. Leuven: Leuven University Press.

Degryse, P., & Schneider, J. (2008). Pliny the Elder and Sr–Nd isotopes: Tracing the provenance of raw materials for Roman glass production. *Journal of Archaeological Science*, *35*, 1993–2000.

Dussart, O. (1998). *Le verre en Jordanie et en Syrie du Sud* (Vol. *152*). Bierut: Institut Français d'Archéologie du Proche-Orient.

Fischer, A., & McGray, W. P. (1999). Glass production activities as practised at Sepphoris, Israel (37 BC–AD 1516). *Journal of Archaeological Science*, *26*(8), 893–905.

Foy, D., Picon, M., Vichy, M., & Thirion-Merle, V. (2003). Caracterisation des verres de la fin de l'Antiquité en Mediterranée occidentale: L'emergence de nouveaux courants commerciaux. In D. Foy & M.-D. Nenna (Eds.), *Echanges et commerce du verre dans le monde antique: Actes du Colloque de l'Association Française pour l'Archéologie du Verre, Aix-en-Provence et Marseille, 7–9 juin 2001* (pp. 41–86). Montagnac: Editions Monique Mergoil.

Freestone, I. C. (2015). The recycling and reuse of Roman glass: Analytical approaches. *Journal of Glass Studies*, *57*, 29–40.

Freestone, I. C. (in press). Glass production in the first millennium CE: A compositional perspective. In F. Klimscha, H. J. Karlsen, S. Hansen, & J. Renn (Eds.), *Glas und Glasproduktion in Ur- und Frühgeschichtlicher Zeit*. Edition TOPOI.

Freestone, I. C., Gorin-Rosen, Y., & Hughes, M. J. (2000). Primary glass from Israel and the production of glass in late antiquity and the Early Islamic period. *Travaux de la Maison de l'Orient Méditerranéen*, *33*, 65–83.

Freestone, I. C., Ponting, M., & Hughes, M. J. (2002). The origins of Byzantine glass from Maroni Petrera, Cyprus. *Archaeometry*, *44*(2), 257–272.

Freestone, I. C., Leslie, K. A., Thirlwall, M., & Gorin-Rosen, Y. (2003). Strontium isotopes in the investigation of early glass production: Byzantine and Early Islamic glass from the Near East. *Archaeometry*, *45*(1), 19–32.

Freestone, I. C., Jackson-Tal, R. E., & Tal, O. (2008). Raw glass and the production of glass vessels at late Byzantine Apollonia-Arsuf, Israel. *Journal of Glass Studies*, *50*, 67–80.

Freestone, I. C., Degryse, P., Lankton, J., Gratuze, B., & Schneider, J. (2018). HIMT, glass composition and commodity branding in the primary glass industry. In D. Rosenow, M. Phelps, A. Meek, & I. C. Freestone (Eds.), *Things that travelled: Glass in the first millennium CE*. London: UCL Press.

Freestone, I. C., & Stapleton, C. P. (2015). Composition, technology and production of colored glasses from Roman mosaic vessels. *Glass of the Roman world* (pp. 61–76). Oxford: Oxbow Books.

Gallo, F., Silvestri, A., Degryse, P., Ganio, M., Longinelli, A., & Molin, G. (2015). Roman and late-Roman glass from north-eastern Italy: The isotopic perspective to provenance its raw materials. *Journal of Archaeological Science*, *62*, 55–65.

Ganio, M., Boyen, S., Brems, D., Scott, R., Foy, D., Latruwe, … Degryse, P. (2012). Trade routes across the Mediterranean: A Sr/Nd isotopic investigation on Roman colourless glass. *Glass Technology-European Journal of Glass Science and Technology Part A*, *53*, 217–224.

Gogebakan, Z., & Selçuk, N. (2009). Trace elements partitioning during cofiring biomass with lignite in a pilot-scale fluidized bed combustor. *Journal of Hazardous Materials*, *162*(2), 1129–1134.

Gorin-Rosen, Y. (2000). The ancient glass industry in Israel: Summary of the finds and new discoveries. *Travaux de la Maison de l'Orient Méditerranéen*, *33*(1), 49–63.

Gratuze, B., & Barrandon, J. -N. (1990). Islamic glass weights and stamps: Analysis using nuclear techniques. *Archaeometry*, *32*, 155–162.

Grose, D. F. (2012). The Pre-Hellenistic, Hellenistic, Roman, and Islamic glass vessels Tel Anafa II, ii. In A. M. Berlin & S. C. Herbert (Eds.), *Glass vessels, lamps, objects of metal, and groundstone and other stone tools and vessels* (pp. 1–98). Ann Arbor: Kelsey Museum Publications.

Hadad, S. (2005). *Islamic glass vessels from the Hebrew University excavations at Bet Shean*. Jerusalem: Monographs of the Institute of Archaeology.

Hayes, J. W. (1975). *Roman and pre-Roman glass in the Royal Ontario Museum: A catalogue*. Toronto: Royal Ontario Museum.

Israeli, Y. (2003). *Ancient glass in the Israel Museum: The Eliahu Dobkin collection and other gifts*. Jerusalem: The Israel Museum.

Jackson, C. M. (1996). From Roman to Early Medieval glasses: Many happy returns or a new birth? *Annales Du 13e Congr*, 289–302.

Jackson, C. M. (2005). Making colourless glass in the Roman period. *Archaeometry*, *47*(4), 763–780.

Jackson, C. M., & Paynter, S. (2016). Great big melting pot. Exploring patterns of glass supply, consumption and recycling in Roman Coppergate, York. *Archaeometry*, *58*(1), 68–95.

Jackson, C. M., Paynter, S., Nenna, M. D., & Degryse, P. (2016). Glassmaking using natron from el-Barnugi (Egypt): Pliny and the Roman glass industry. *Archaeological and Anthropological Sciences*, 1–13.

James, L. (2010). Byzantine mosaics and glass: A problematic relationship. *Glass in Byzantium e Production, Usage, Analyses, RGZM e Tagung*, *8*, 237–243.

Jennings, S. (2006). Vessel glass from Beirut: BEY 006, 007 and 045. *Berytus Archaeological Studies*, *48–49*, 2004–2005.

Kakhidze, A., & Shalikadze, T. (2009). *Pichvnari 4: Glassware from the southwestern littorial of Georgia: Results of excavations conducted by the N. Berdzenishvili Batumi Research Institute and the Joint British-Georgian Pichvnari expeditions 1967–2008*. Oxford: Oxbow Books.

Kamber, B. S., Greig, A., & Collerson, K. D. (2005). A new estimate for the composition of weathered young upper continental crust from alluvial sediments, Queensland, Australia. *Geochimica et Cosmochimica Acta*, *69*(4), 1041–1058.

Keller, D. (2006). *Petra Ez-Zantur III, Ergebnisse der Schweizerisch-Liechtensteinischen Ausgrabungen. Teil 1: Die gläser aus Petra*. Mainz: Verlag Philipp von Zabern.

Kraeling, C. H. (1938). *Gerasa, city of the Decapolis: An account embodying the record of a joint excavation conducted by Yale University and the British School of Archaeology in Jerusalem (1928–1930), and Yale University and the American Schools of Oriental Research (1930–1931, 1933–1934)*. New Haven: American Schools of Oriental Research.

Lichtenberger, A., & Raja, R. (2015). New archaeological research in the Northwest Quarter of Jerash and its implications for the urban development of Roman Gerasa. *American Journal of Archaeology*, *119*, 483–500.

Lichtenberger, A., & Raja, R. (2017). *Gerasa/Jerash. from the urban periphery*. Aarhus: AUTRYK.

Lightfoot, C. S. (2007). *Ancient glass in the National Museums Scotland*. Edinburgh: NMS Enterprises Ltd.

Lilyquist, C., Brill, R. H., & Wypyski, M. T. (1993). *Studies in early Egyptian glass*. Metropolitan Museum of Art.

Marii, F., & Rehren, T. (2009). Archaeological colored glass cakes and tesserae from the Petra church. *Annales 17e Congrès de l'Association Internationale pour l'Histoire du Verre* (pp. 295–300). Antwerp: University Press Antwerp.

Metrich, N., & Rutherford, M. J. (1992). Experimental study of chlorine behavior in hydrous silicic melts. *Geochimica et Cosmochimica Acta*, *56*, 607–616.

Meyer, C. (1988). Glass from the North Theater Byzantine church, and soundings at Jerash, Jordan, 1982–1983. In W. E. Rast (Ed.), *Preliminary reports of ASOR-sponsored excavations, 1982–85* (pp. 175–222). Baltimore: Johns Hopkins University Press for the American Schools of Oriental Research.

Miranda, T., Esteban, A., Rojas, S., Montero, I., & Ruiz, A. (2008). Combustion analysis of different olive residues. *International Journal of Molecular Sciences*, *9*(4), 512–525.

Mirti, P., Lepora, A., & Saguì, L. (2000). Scientific analysis of Seventh-Century glass fragments from the Crypta Balbi in Rome. *Archaeometry*, *42*(2), 359–374.

Misra, M. K., Ragland, K. W., & Baker, A. J. (1993). Wood ash composition as a function of furnace temperature. *Biomass and Bioenergy*, *4*(2), 103–116.

Molina, J. F., Scarrow, J. H., Montero, P. G., & Bea, F. (2009). High-Ti amphibole as a petrogenetic indicator of magma chemistry: Evidence for mildly alkalic-hybrid melts during evolution of Variscan basic–ultrabasic magmatism of Central Iberia. *Contributions to Mineralogy and Petrology*, *158*(1), 69–98.

Möncke, D., Papageorgiou, M., Winterstein-Beckmann, A., & Zacharias, N. (2014). Roman glasses colored by dissolved transition metal ions: Redox-reactions, optical spectroscopy and ligand field theory. *Journal of Archaeological Science*, *46*, 23–36.

Nenna, M.-D., Vichy, M., & Picon, M. (1997). L'Atelier de verrier de Lyon, du Ier siècle après J.-C., et l'origine des verres Romains. *Revue d'Archèomètrie*, *21*, 81–87.

Oliver, A. (1980). *Ancient glass in the Carnegie Museum of Natural History, Pittsburgh*. Pittsburgh: Carnegie Institute.

Paynter, S. (2008). Experiments in the reconstruction of Roman wood-fired glassworking furnaces: Waste products and their formation processes. *Journal of Glass Studies*, *50*, 271–290.

Phelps, M., Freestone, I. C., Gorin-Rosen, Y., & Gratuze, B. (2016). Natron glass production and supply in the late antique and early medieval Near East: The effect of the Byzantine-Islamic transition. *Journal of Archaeological Science*, *75*, 57–71.

Pollak, R. (2006). The glass. In R. R. Stieglitz (Ed.), *Tel Tanninim. Excavations at Krokodeilon Polis 1996–1999* (pp. 155–193). Boston: American Schools of Oriental Research.

Reade, W. J., & Privat, K. L. (2016). Chemical characterisation of archaeological glasses from the Hellenistic site of Jebel Khalid, Syria by electron probe microanalysis. *Heritage Science*, *4*(1), 1–17.

Rehren, T., & Freestone, I. C. (2015). Ancient glass: From kaleidoscope to crystal ball. *Journal of Archaeological Science*, *56*, 233–241.

Rehren, T., Marii, F., Schibille, N., Stanford, L., & Swan, C. (2010). Glass supply and circulation in early Byzantine southern Jordan. In J. Drauschke & D. Keller (Eds.), *Glas in Byzanz: Produktion, Verwendung, Analysen, Mainz, RGAM Tagungen Band 8* (pp. 65–81). Mainz: Verlag des Römisch-Germanischen Zentralmuseums.

Rowan, E. (2015). Olive oil pressing waste as a fuel source in antiquity. *American Journal of Archaeology*, *119*(4), 465–482.

Sayre, E. V. (1963). The intentional use of antimony and manganese in ancient glasses. In F. R. Matson & G. E. Rindone (Eds.), *Advances in glass technology* (pp. 263–282, Part 2). New York: Plenum Press.

Sayre, E. V., & Smith, R. W. (1961). Compositional categories of ancient glass. *Science*, *133*, 1824–1826.

Schalm, O., Janssens, K., Wouters, H., & Caluwé, D. (2007). Composition of 12–18th century window glass in Belgium: Non-figurative windows in secular buildings and stained-glass windows in religious buildings. *Spectrochimica Acta Part B: Atomic Spectroscopy*, *62*(6), 663–668.

Schalm, O., Proost, K., De Vis, K., Cagno, S., Janssens, K., Mees, F., … Caen, J. (2011). Manganese staining of archaeological glass: The characterization of Mn-rich inclusions in leached layers and a hypothesis of its formation. *Archaeometry*, *53*(1), 103–122.

Schibille, N., Sterrett-Krause, A., & Freestone, I. C. (2017). Glass groups, glass supply and recycling in late Roman Carthage. *Archaeological and Anthropological Sciences*, *9*(6), 1223–1241.

Schreurs, J. W. H., & Brill, R. H. (1984). Iron and sulphur-related colours in ancient glass. *Archaeometry*, *16*, 199–209.

Schwarzer, H. (2009a). Spätantike und byzantinische Glasfunde aus Alexandreia Troas. In E. Laflı (Ed.), *Istanbul, in Late Antiquity/Early Byzantine glass in the Eastern Mediterranean* (pp. 67–84). Izmir: Tübitak.

Schwarzer, H. (2009b). Spätantike, byzantinische und islamische Glasfunde aus Pergamon. In E. Laflı (Ed.), *Istanbul, in Late Antiquity/Early Byzantine glass in the Eastern Mediterranean* (pp. 85–109). Izmir: Tübitak.

Schwarzer, H. (2014). Glass finds. In A. Lichtenberger, R. Raja, & A.H. Sørensen (Eds.), The Danish–German Jerash Northwest Quarter Project 2013. Preliminary Registration Report. *Annual of the Department of Antiquities of Jordan*, *58*(48 f. 88), 91–95.

Shepherd, J. D. (1999). The glass. In A. G. Poulter (Ed.), *Nicopolis ad Istrum: A Roman to Early Byzantine city* (pp. 297–378). London: Leicester University Press for the Society of Antiquaries of London.

Silvestri, A. (2008). The colored glass of Iulia Felix. *Journal of Archaeological Science*, *35*, 1489–1501.

Silvestri, A., Molin, G., & Salviulo, G. (2008). The colourless glass of Iulia Felix. *Journal of Archaeological Science*, *35*(2), 331–341.

Stern, E. M. (2001). *Römisches, byzantinisches und frühmittelalterliches Glas*. Berlin: Hatje Cantz Verlag.

Tal, O., Jackson-Tal, R. E., & Freestone, I. C. (2004). New evidence of the production of raw glass at late Byzantine Apollonia-Arsuf, Israel. *Journal of Glass Studies*, *46*, 51–66.

Tal, O., Jackson-Tal, R. E., & Freestone, I. C. (2008). Glass from a Late Byzantine secondary workshop at Ramla (south), Israel. *Journal of Glass Studies*, *50*, 81–95.

von Saldern, A. (1974). *Glassammlung Hentrich: Antike und Islam*. Düsseldorf: Kunstmuseum Düsseldorf.

von Saldern, A. (1980). *Ancient and Byzantine glass from Sardis* (Archaeological Exploration of Sardis, Vol. 6). Cambridge: Harvard University Press.

Veksler, I. V., Dorfman, A. M., Dulski, P., Kamenetsky, V. S., Danyushevsky, L. V., Jeffries, T., & Dingwell, D. B. (2012). Partitioning of elements between silicate melt and immiscible fluoride, chloride, carbonate, phosphate and sulfate melts, with implications to the origin of natrocarbonatite. *Geochimica et Cosmochimica Acta*, *79*, 20–40.

Vicenzi, E. P., Eggins, S., Logan, A., & Wysoczanski, R. (2002). Microbeam characterization of corning archeological reference glasses: New additions to the smithsonian microbeam standard collection. *Journal of Research of the National Institute of Standards and Technology*, *107*(6), 719–727.

Wagner, B., Nowak, A., Bulska, E., Hametner, K., & Günther, D. (2012). Critical assessment of the elemental composition of Corning archeological reference glasses by LA-ICP-MS. *Analytical and Bioanalytical Chemistry*, *402*(4), 1667–1677.

Walmsley, A. (2000). Production, exchange and regional trade in the Islamic East Mediterranean: Old structures, new systems? In I. L. Hansen & C. Wickham (Eds.), *The long eighth century. Production, distribution and demand* (pp. 265–343). Leiden: Brill.

Wardle, A. (2015). *Glass working on the margins of Roman London: Excavations at 35 Basinghall Street, City of London, 2005 (MOLA Monograph 70)*. London: Museum of London Archaeology.

Wedepohl, K. H. (2003). *Glas in Antike und Mittelalter*. Stuttgart: Schweizerbart.

Weinberg, G. D. (1988). *Excavations at Jalame*. Site of a glass factory in Late Roman Palestine: Excavations conducted by a joint expedition of the University of Missouri and the Corning Museum of Glass. Columbia: University of Missouri Press.

Weinberg, G. D., & Stern, E. M. (2009). Vessel glass: The Athenian Agora 34. *Gnomon*, *85*, 354–360.

Weis, D., Kieffer, B., Maerschalk, C., Barling, J., de Jong, J., Williams, G. A., … Mahoney, J. B. (2006). High-precision isotopic characterization of USGS reference materials by TIMS and MC-ICP-MS. *Geochemistry, Geophysics, Geosystems*, *7*(8). https://doi.org/10.1029/2006GC001283

Whitehouse, D. (1997). *Roman glass in the Corning Museum of Glass* (Vol. 1). New York: Corning Museum of Glass.

Whitehouse, D. (2001). *Roman glass in the Corning Museum of Glass* (Vol. 2). New York: Corning Museum of Glass.

SUPPORTING INFORMATION

Additional supporting information may be found online in the Supporting Information section at the end of the article.

How to cite this article: Barfod GH, Freestone IC, Lichtenberger A, Raja R, Schwarzer H. Geochemistry of Byzantine and Early Islamic glass from Jerash, Jordan: Typology, recycling, and provenance. *Geoarchaeology*. 2018;33:623–640. https://doi.org/10.1002/gea.21684